Electronic Supplementary Material (ESI) for Journal of Materials Chemistry A.

Selecting Dual Atomic Clusters Supported on Two-dimensional Biphenylene Significant Optimization of Capability to Reduce Carbon Monoxide

Zhongwei Wang,[ab] Zhili Yin,[a] Yan Gao,*[a] Haifeng Wang,*[a] Junfeng Gao*[ab] and Jijun Zhao[b]

[a]*College of Sciences/Xinjiang Production & Construction Corps Key Laboratory of Advanced Energy Storage Materials and Technologies, Shihezi University, Shihezi 832000, China*

[b]*Key Laboratory of Materials Modification by Laser, Ion and Electron Beams (Dalian University of Technology), Ministry of Education, Dalian 116024, China*

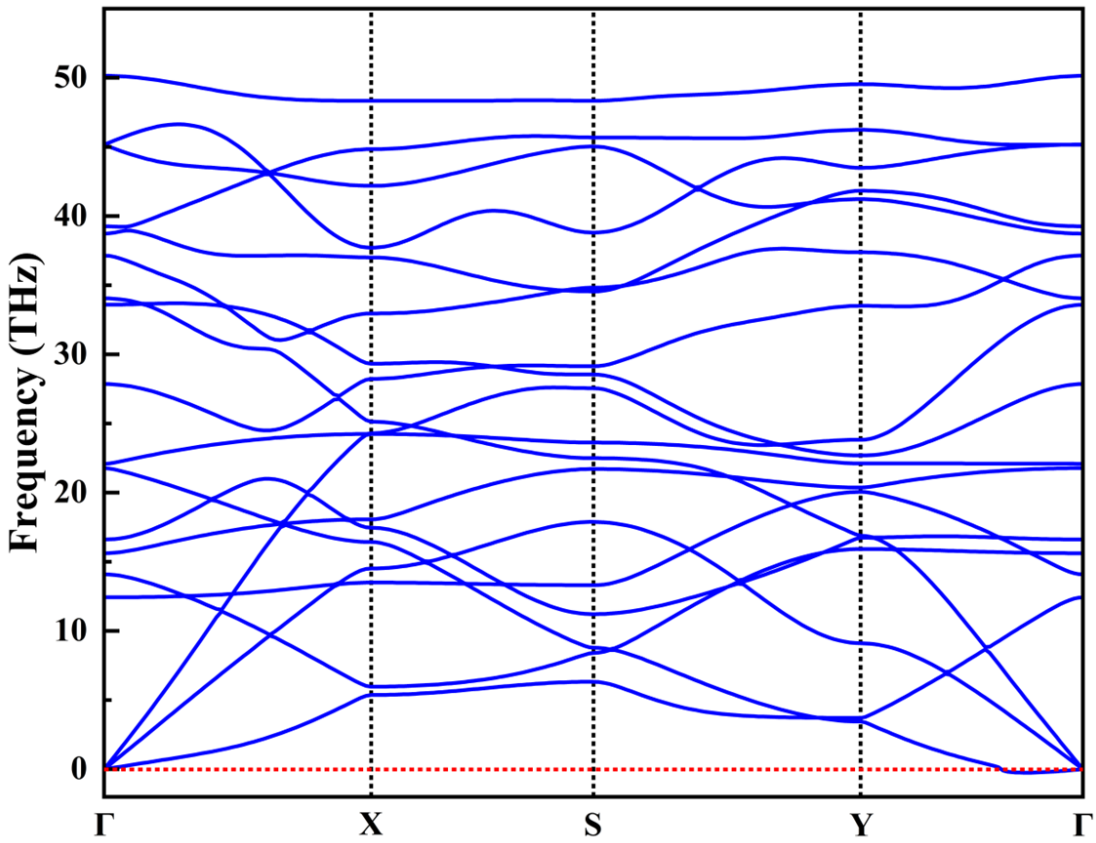

Fig. S1. Phonon dispersion spectrum of the BPN.

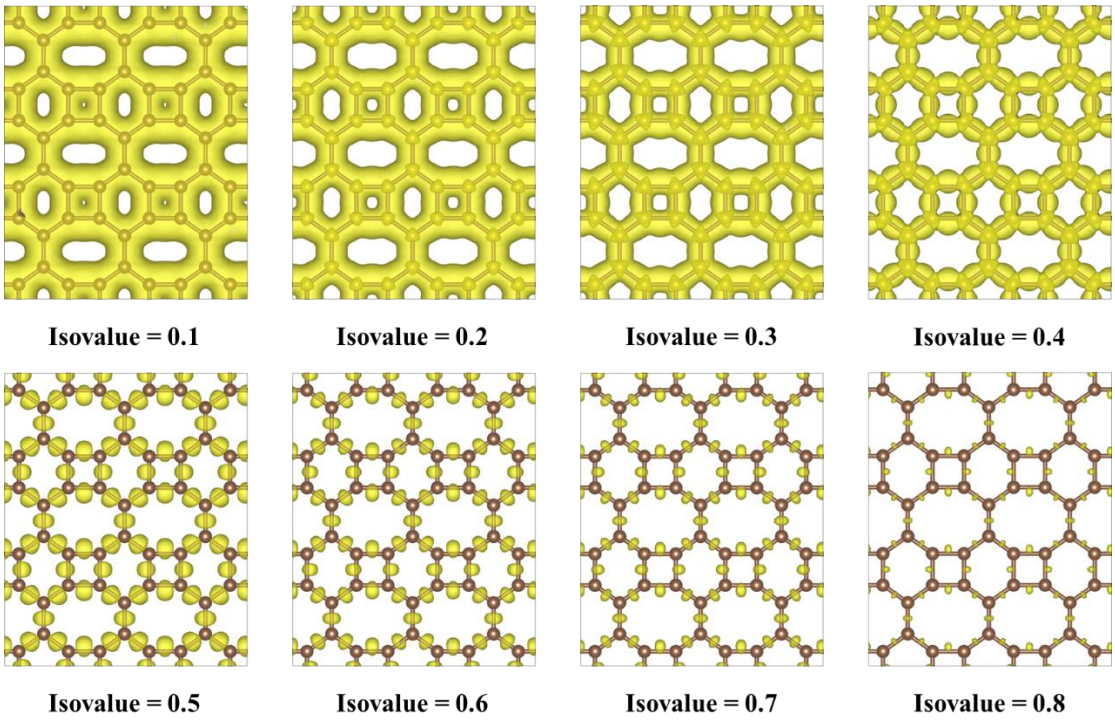

Fig. S2. Isosurfaces of electron localization function of the BPN.

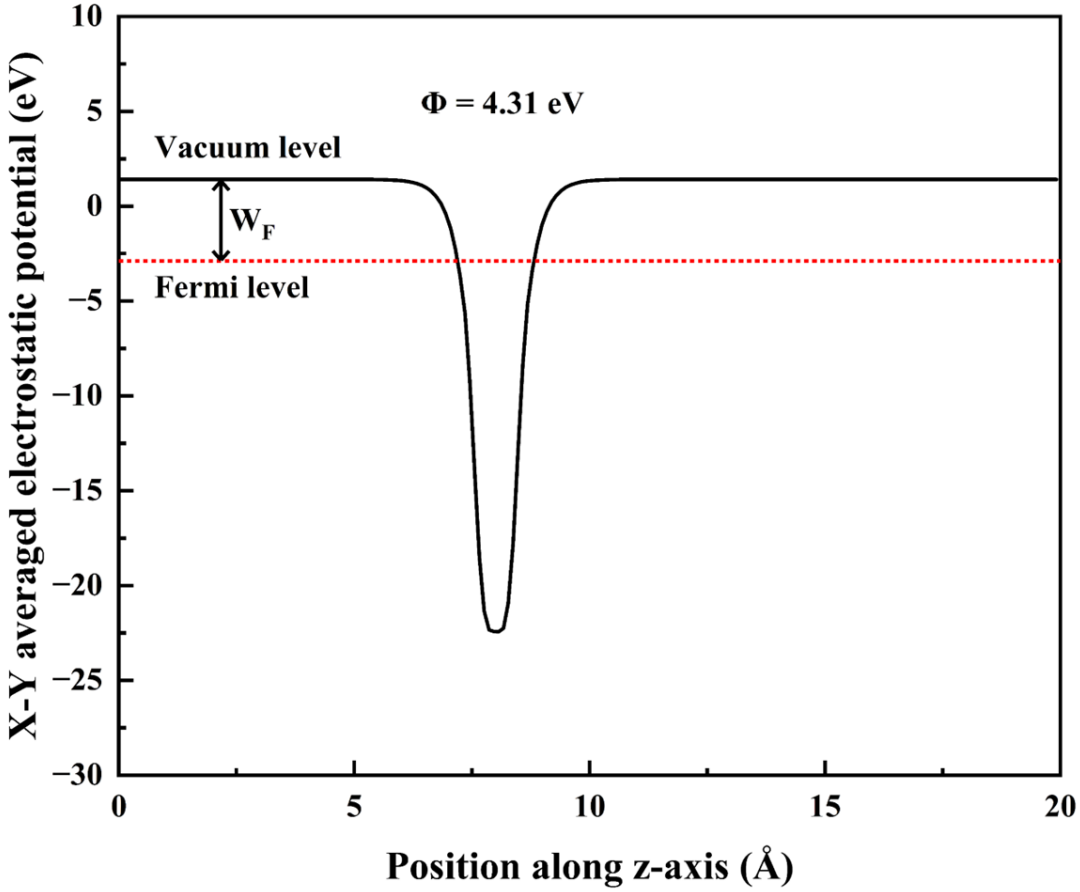

Fig. S3. The electrostatic potential along the z-axis direction.

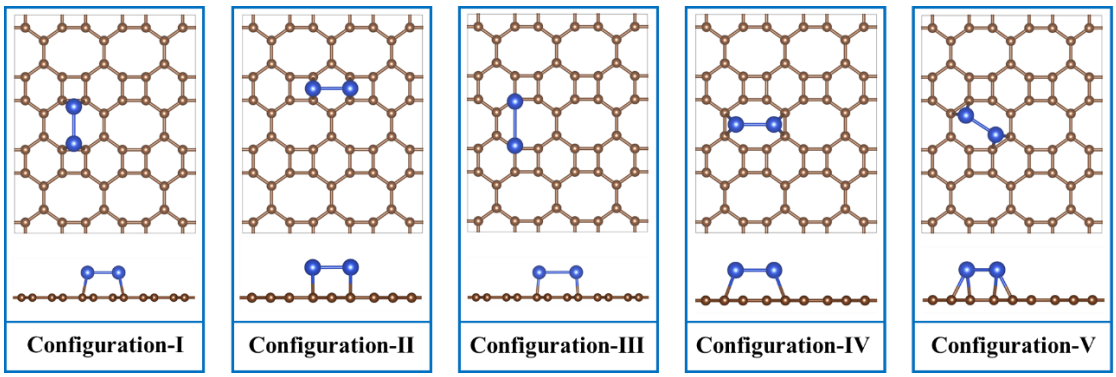

Fig. S4. Five different types of diatomic configurations in BPN.

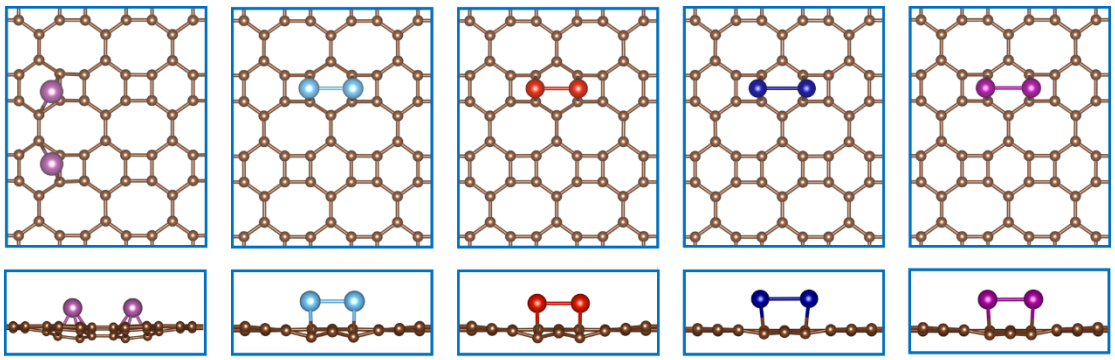

Sc_2@BPN Ti_2@BPN V_2@BPN Cr_2@BPN Mn_2@BPN

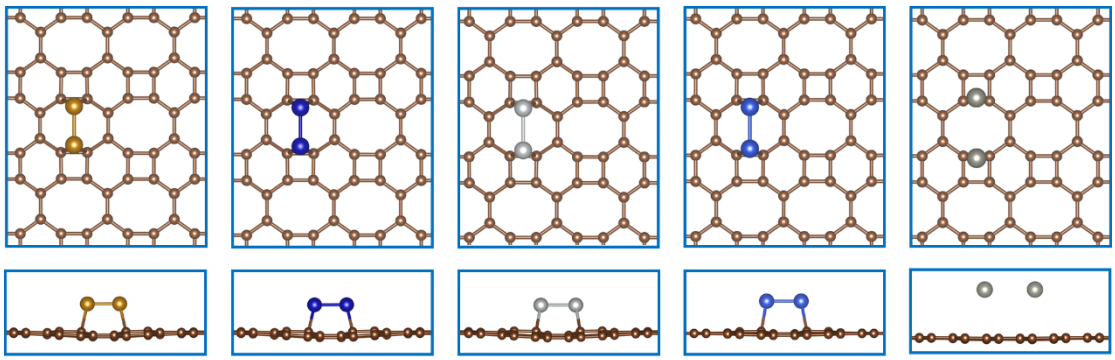

Fe_2@BPN Co_2@BPN Ni_2@BPN Cu_2@BPN Zn_2@BPN

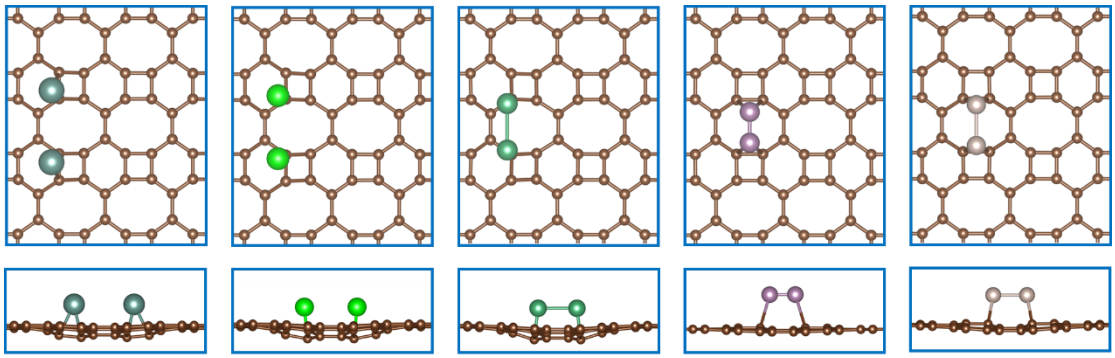

Y_2@BPN Zr_2@BPN Nb_2@BPN Mo_2@BPN Ru_2@BPN

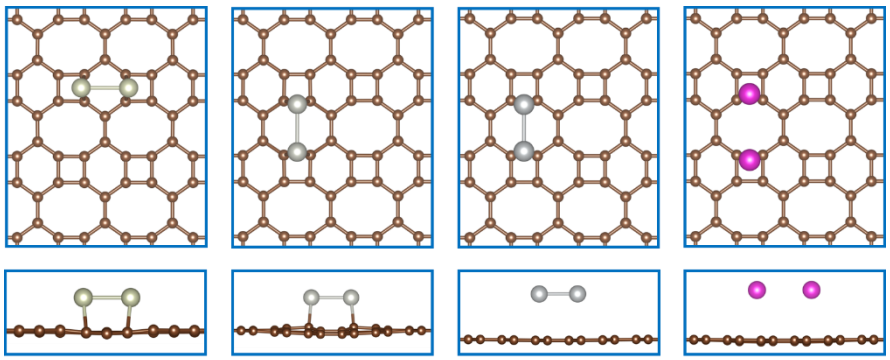

Rh_2@BPN Pd_2@BPN Ag_2@BPN Cd_2@BPN

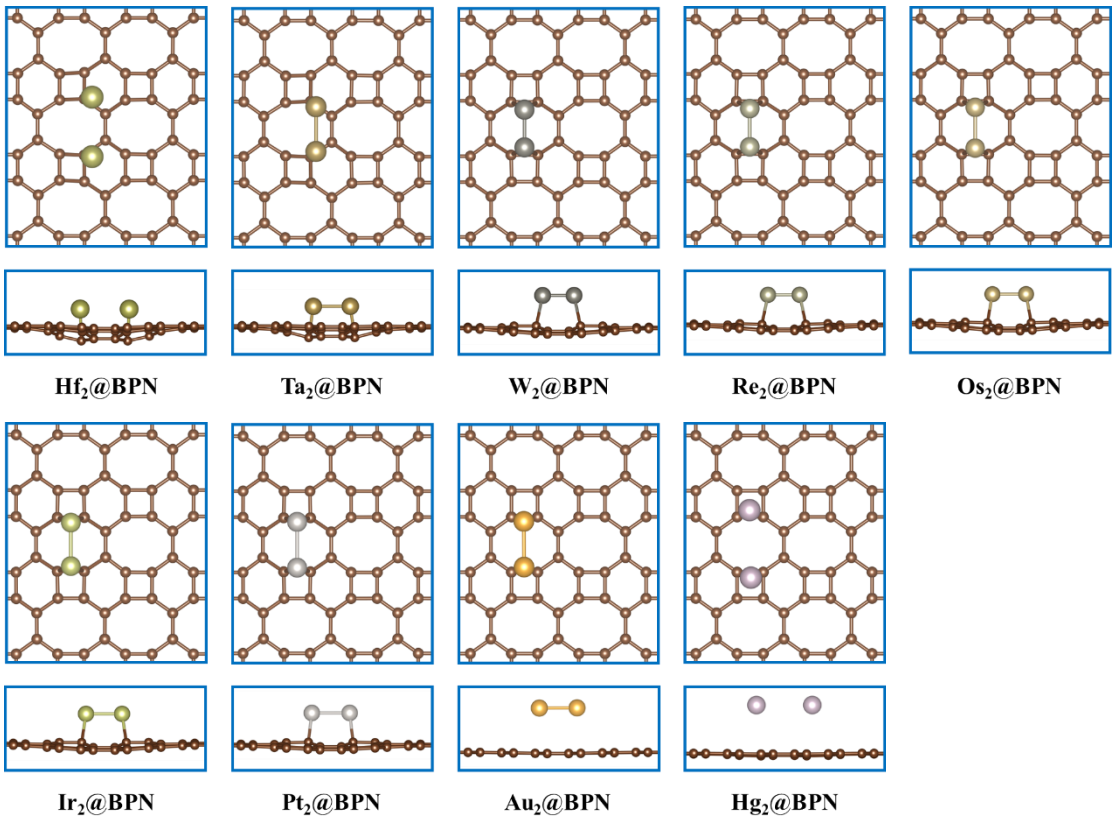

Fig. S5. Optimal adsorption conformations of 3d, 4d, and 5d transition metal diatoms.

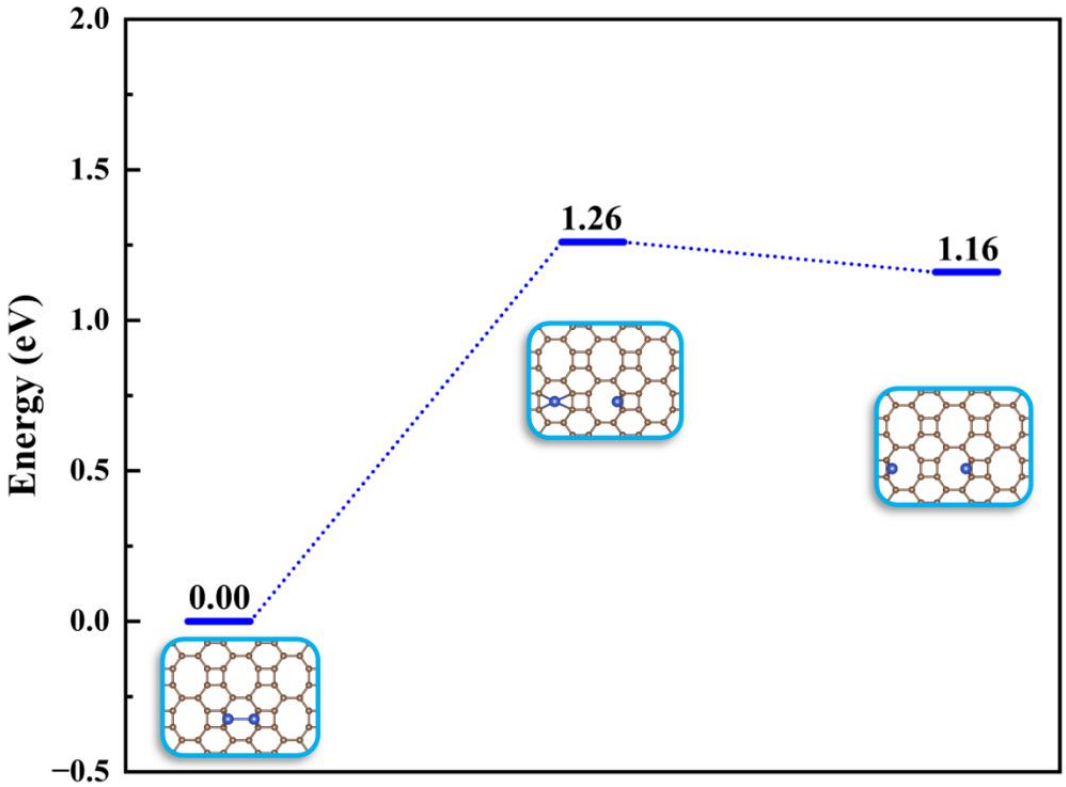

Fig. S6. The calculated migration barrier for Cu.

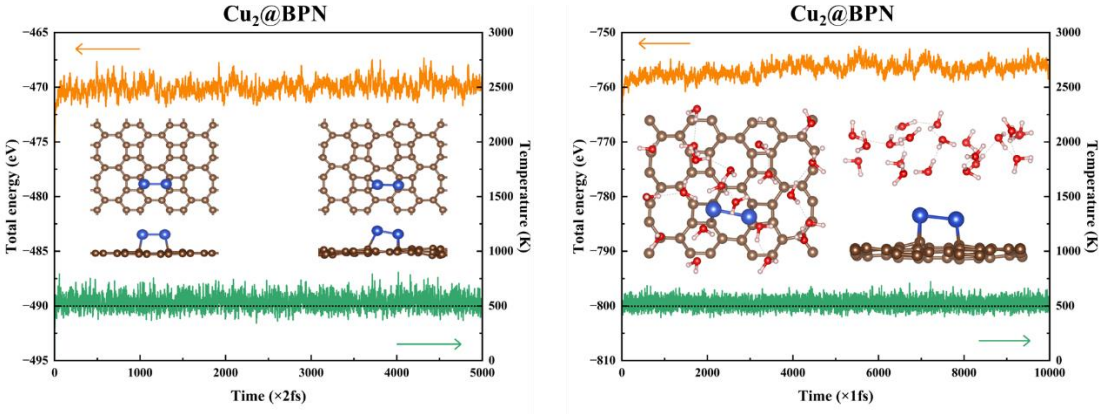

Fig. S7. AIMD simulations of Cu_2BPN were carried out at 500 K over a total time step of 10 ps, using both vacuum conditions and an explicit solvent model to simulate aqueous solution conditions. The green and yellow parts in the figure represent temperature and energy, respectively.

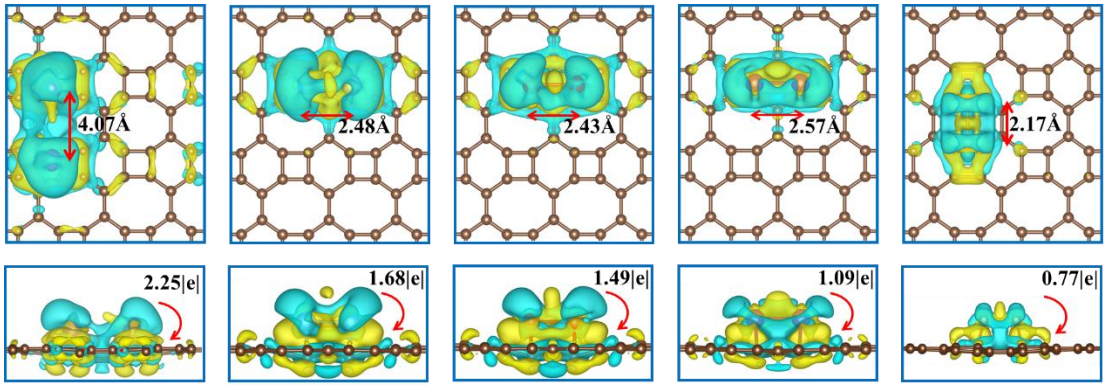

Sc_2@BPN Ti_2@BPN V_2@BPN Mn_2@BPN Fe_2@BPN

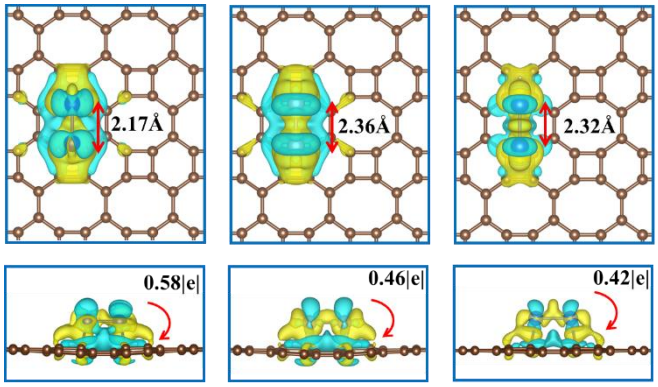

Co_2@BPN Ni_2@BPN Cu_2@BPN

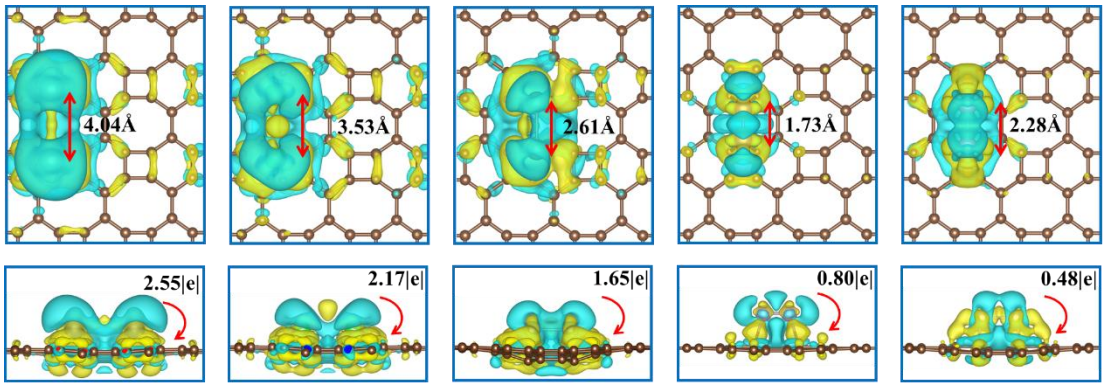

Y_2@BPN Zr_2@BPN Nb_2@BPN Mo_2@BPN Ru_2@BPN

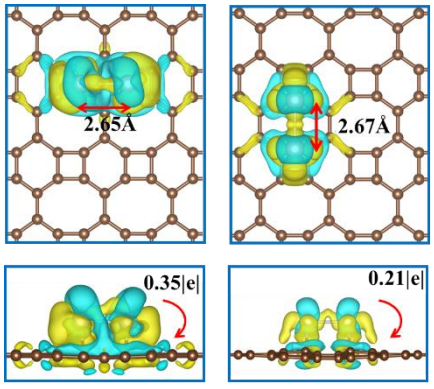

Rh_2@BPN Pd_2@BPN

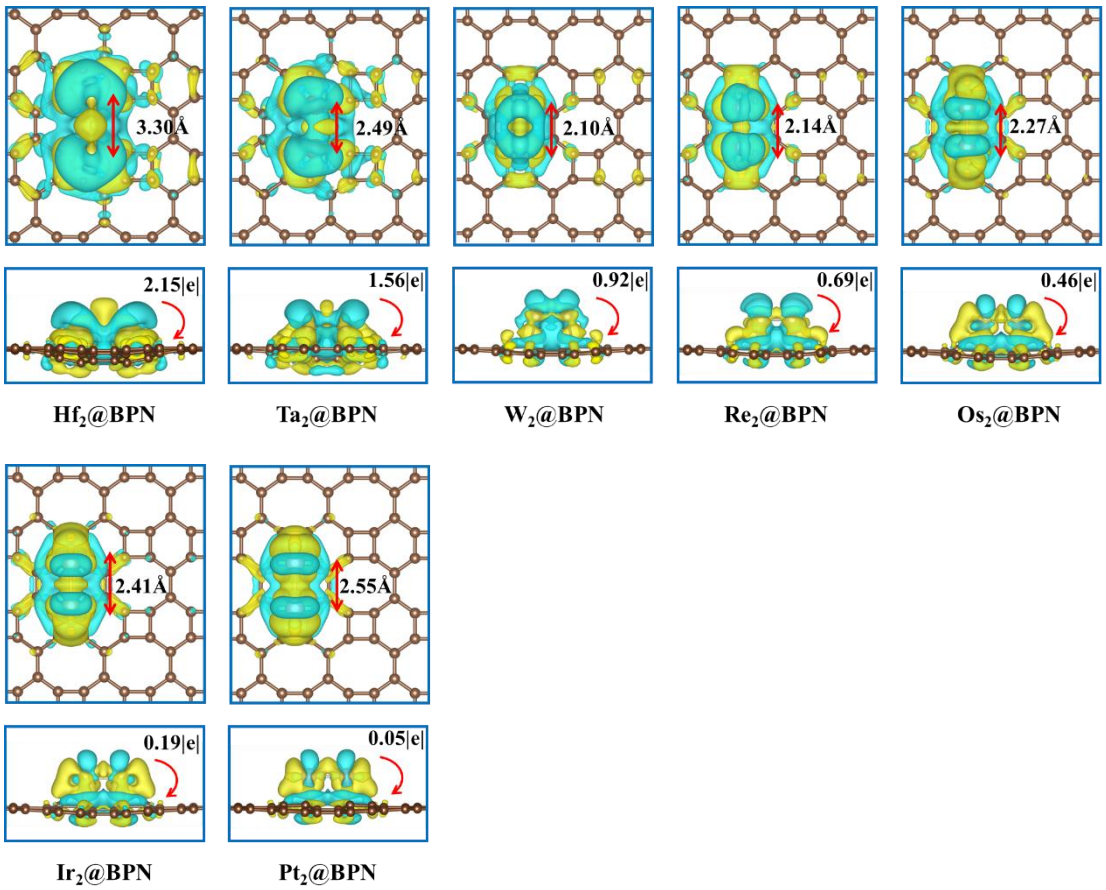

Fig. S8. CDD distributions for 22 TM_2@BPN, where the isosurface value is 0.0015 eÅ^{-3} and cyan and yellow represent the accumulation and depletion of charge, respectively.

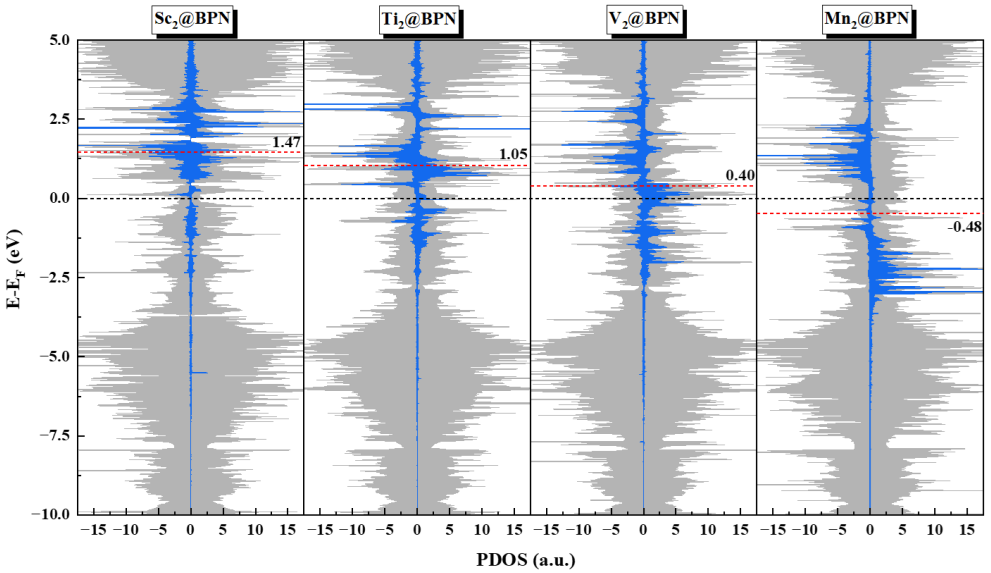
Sc2@BPN
Ti2@BPN
V2@BPN
Mn2@BPN
1.47
1.05
0.40
-0.48
E-EF (eV)
PDOS (a.u.)

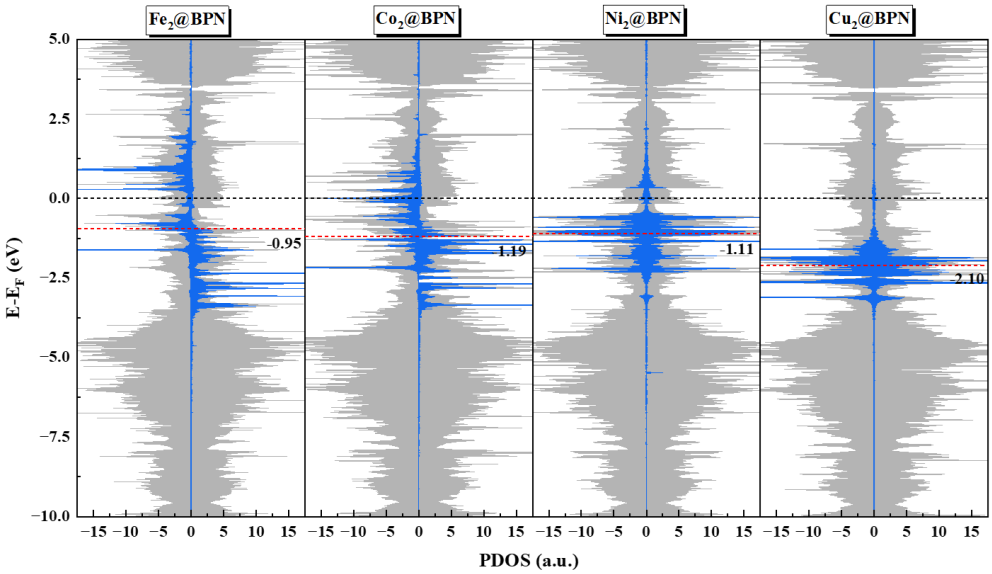
Fe2@BPN
Co2@BPN
Ni2@BPN
Cu2@BPN
-0.95
1.19
1.11
2.10
E-EF (eV)
PDOS (a.u.)

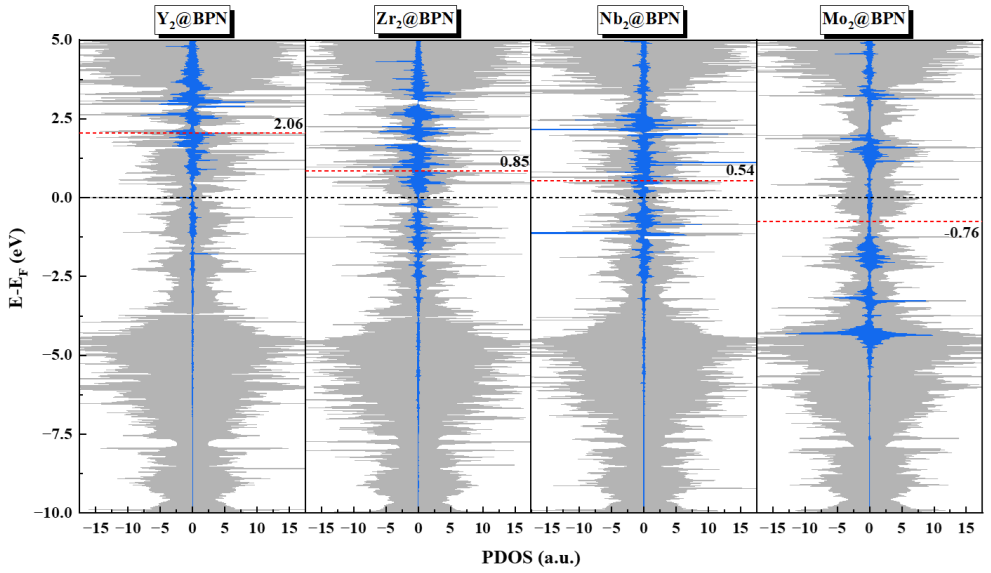
Y2@BPN
Zr2@BPN
Nb2@BPN
Mo2@BPN
2.06
0.85
0.54
-0.76
E-EF (eV)
PDOS (a.u.)

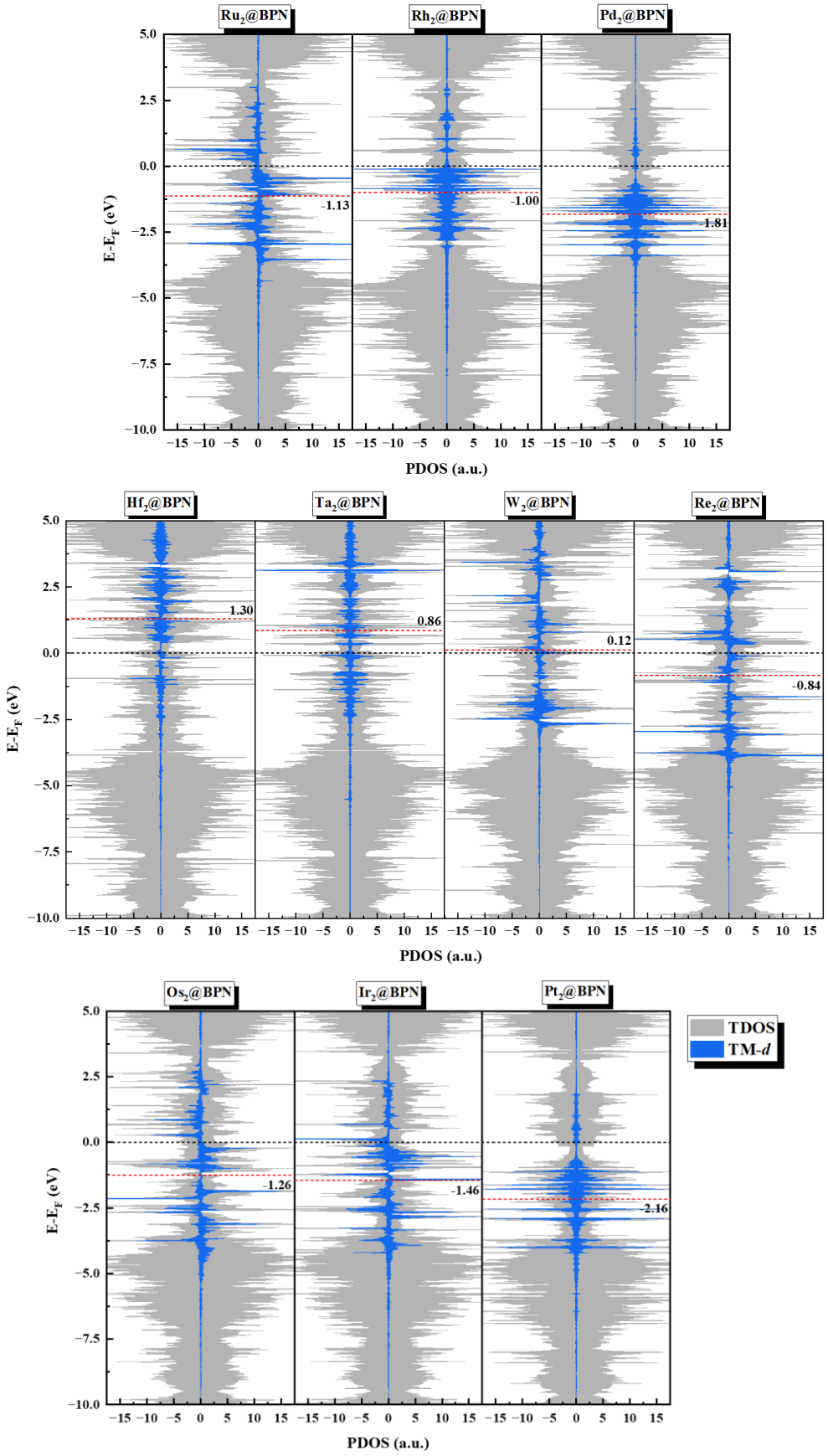

Fig. S9. Calculated the TDOS and *d*-orbital PDOS for 22 TM_2@BPN, displayed in gray and blue, respectively.

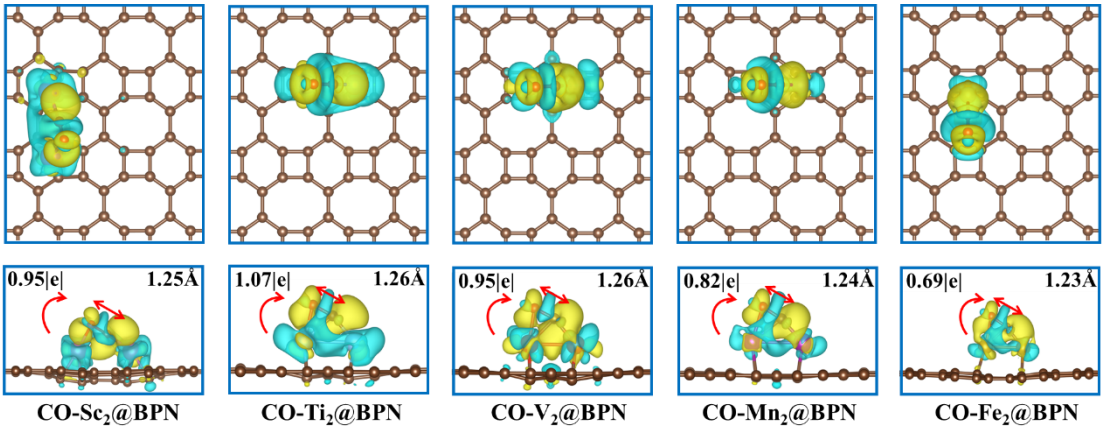

CO-Sc_2@BPN CO-Ti_2@BPN CO-V_2@BPN CO-Mn_2@BPN CO-Fe_2@BPN

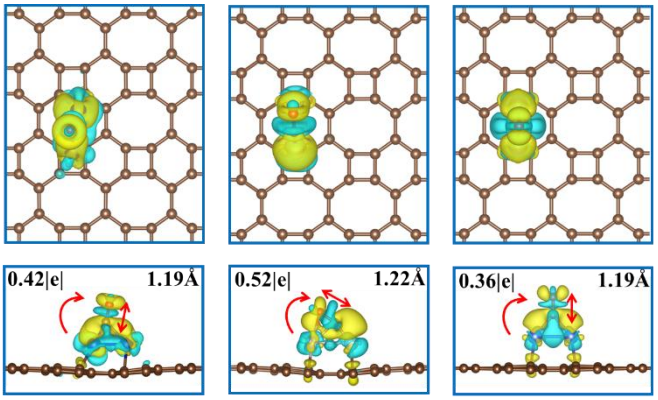

CO-Co_2@BPN CO-Ni_2@BPN CO-Cu_2@BPN

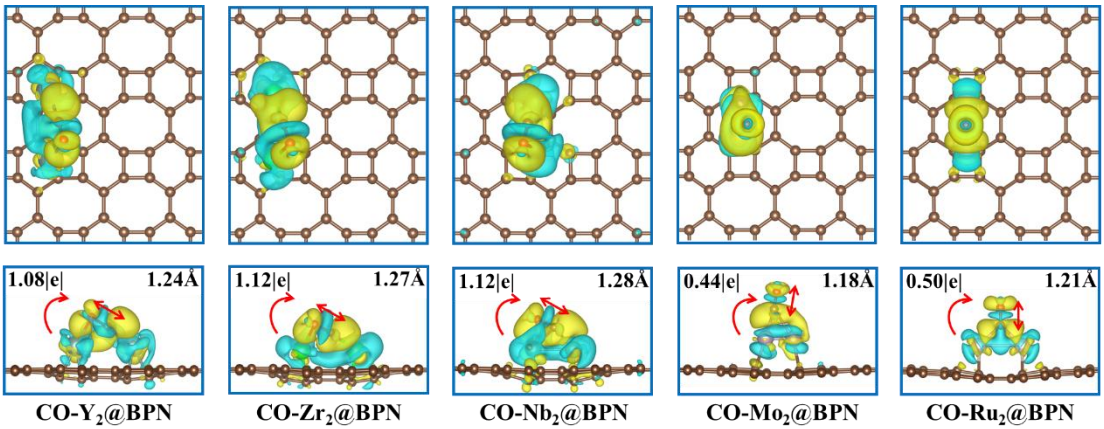

CO-Y_2@BPN CO-Zr_2@BPN CO-Nb_2@BPN CO-Mo_2@BPN CO-Ru_2@BPN

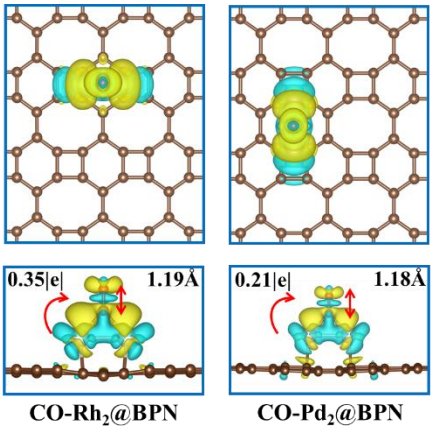

CO-Rh_2@BPN CO-Pd_2@BPN

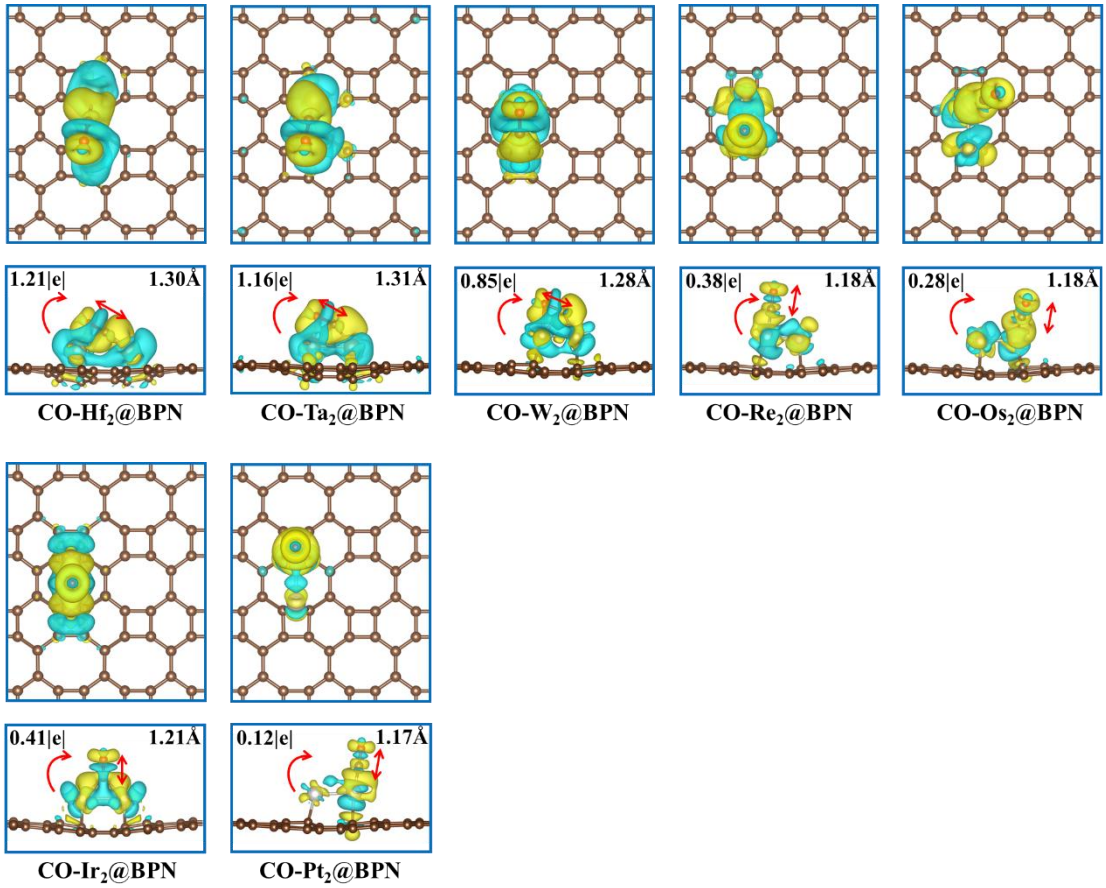

Fig. S10. CDD distributions for 22 CO-TM_2@BPN catalysts, with an isosurface value set at 0.0015 $eÅ^{-3}$. In these distributions, cyan and yellow indicate the accumulation and depletion of charge, respectively

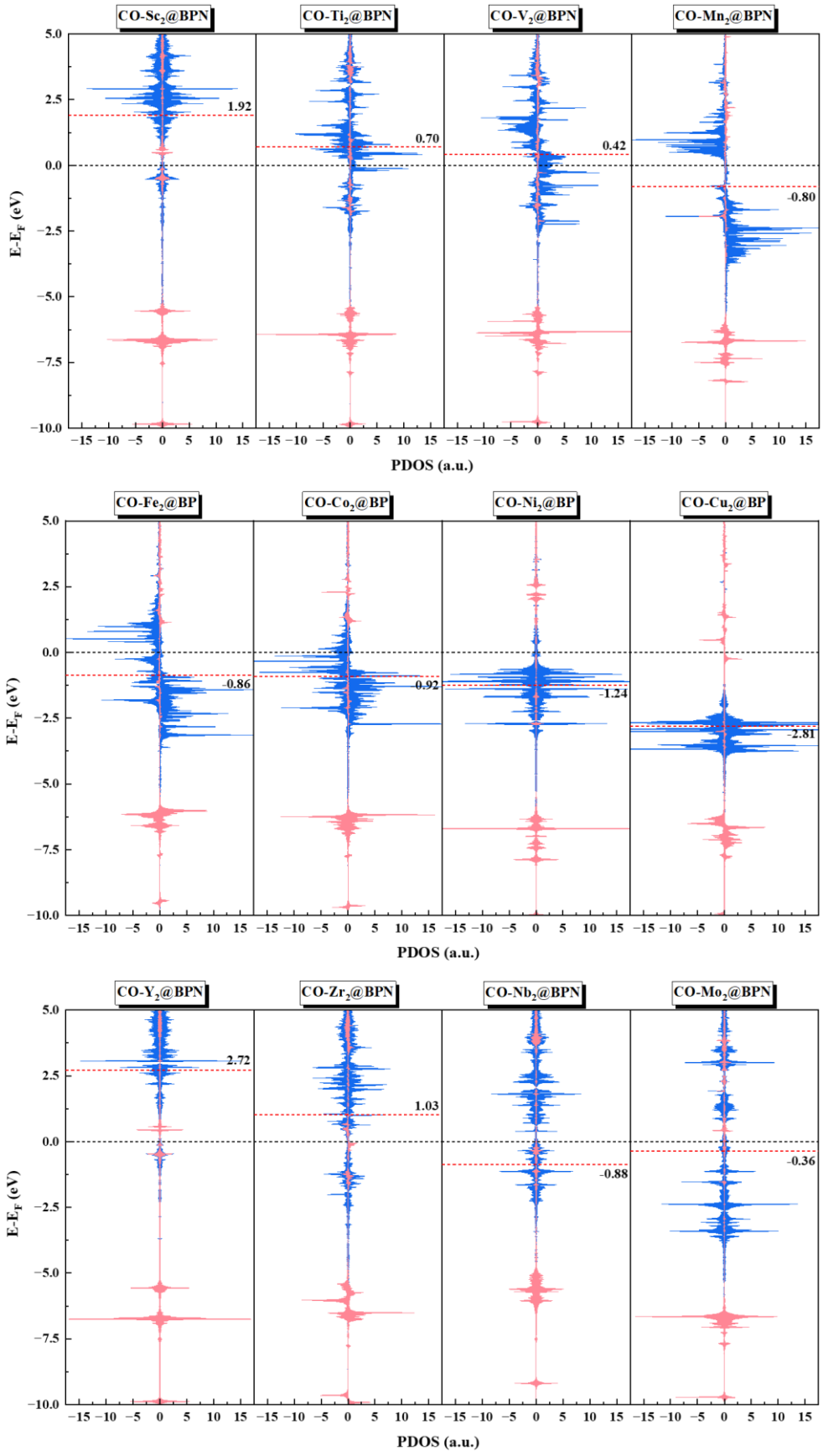
CO-Sc2@BPN
CO-Ti2@BPN
CO-V2@BPN
CO-Mn2@BPN
1.92
0.70
0.42
-0.80
CO-Fe2@BP
CO-Co2@BP
CO-Ni2@BP
CO-Cu2@BP
-0.86
0.92
-1.24
-2.81
CO-Y2@BPN
CO-Zr2@BPN
CO-Nb2@BPN
CO-Mo2@BPN
2.72
1.03
-0.88
-0.36
E-EF (eV)
PDOS (a.u.)

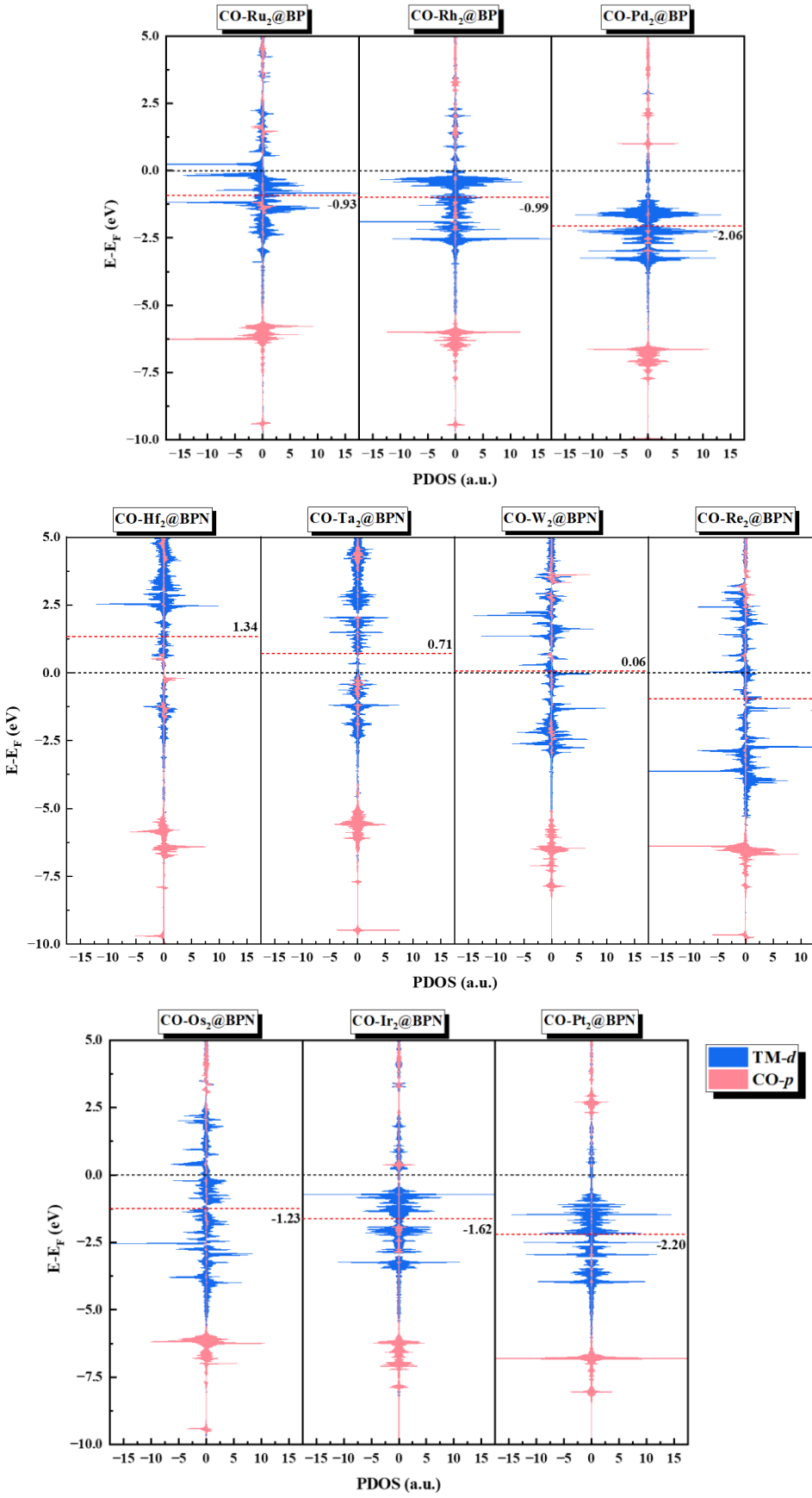

Fig. S11. PDOS calculations for CO molecules on 22 TM_2@BPN surfaces. The *d*-orbitals of TM and the *p*-orbitals of CO are depicted in blue and pink, respectively.

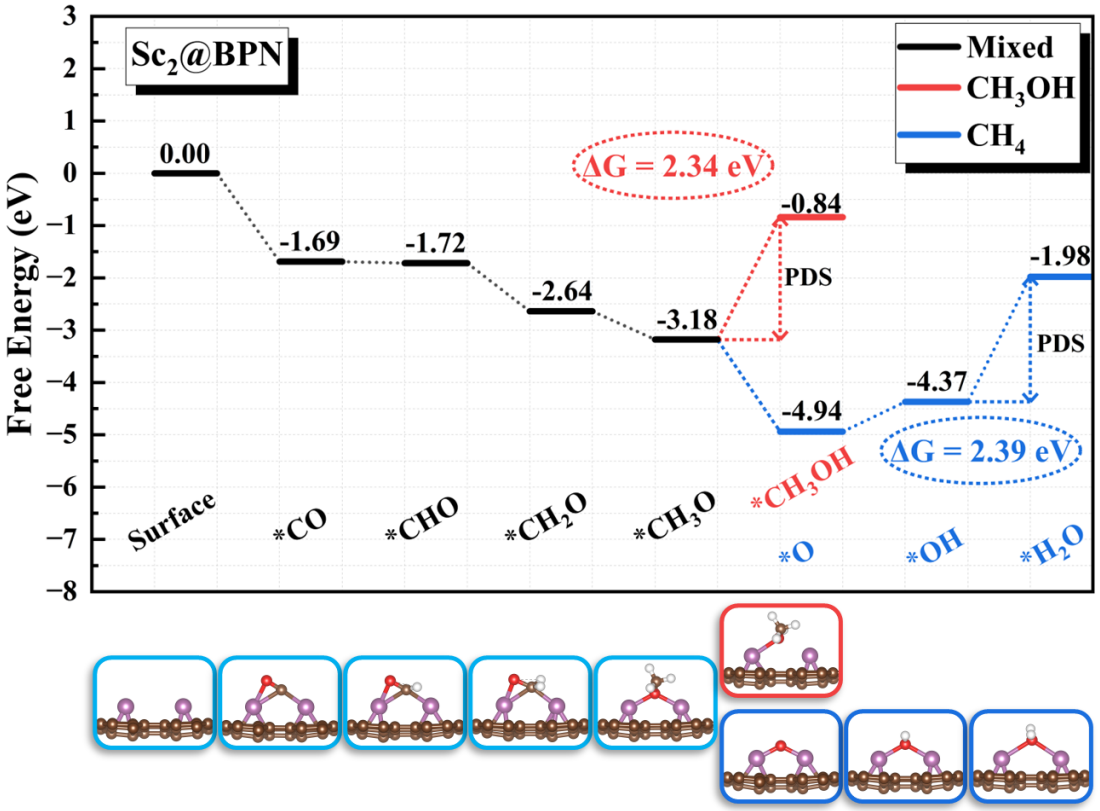

Fig. S12. Free energy diagram of CO reduction to various C_1 on Sc_2@BPN. The black line represents the common path, the red line represents the CH_3OH path, and the blue line represents the CH_4 path.

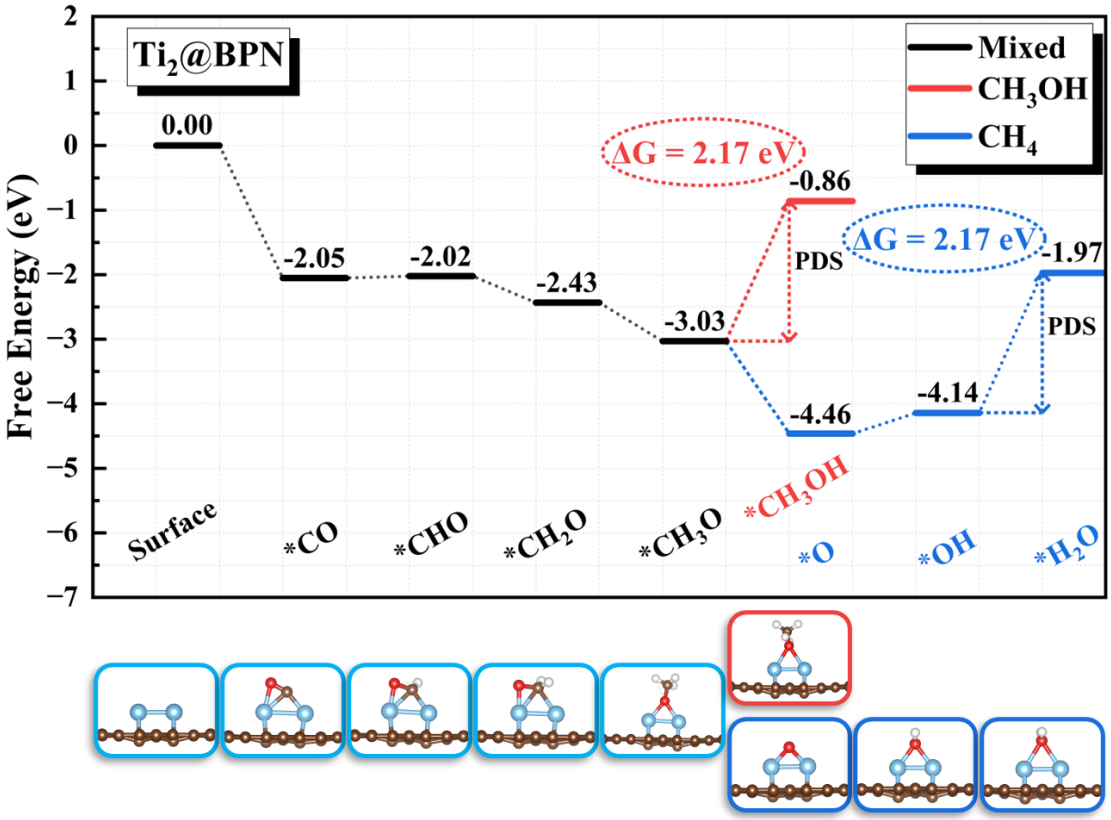

Fig. S13. Free energy diagram of CO reduction to various C_1 on Ti_2@BPN. The black line represents the common path, the red line represents the CH_3OH path, and the blue line represents the CH_4 path.

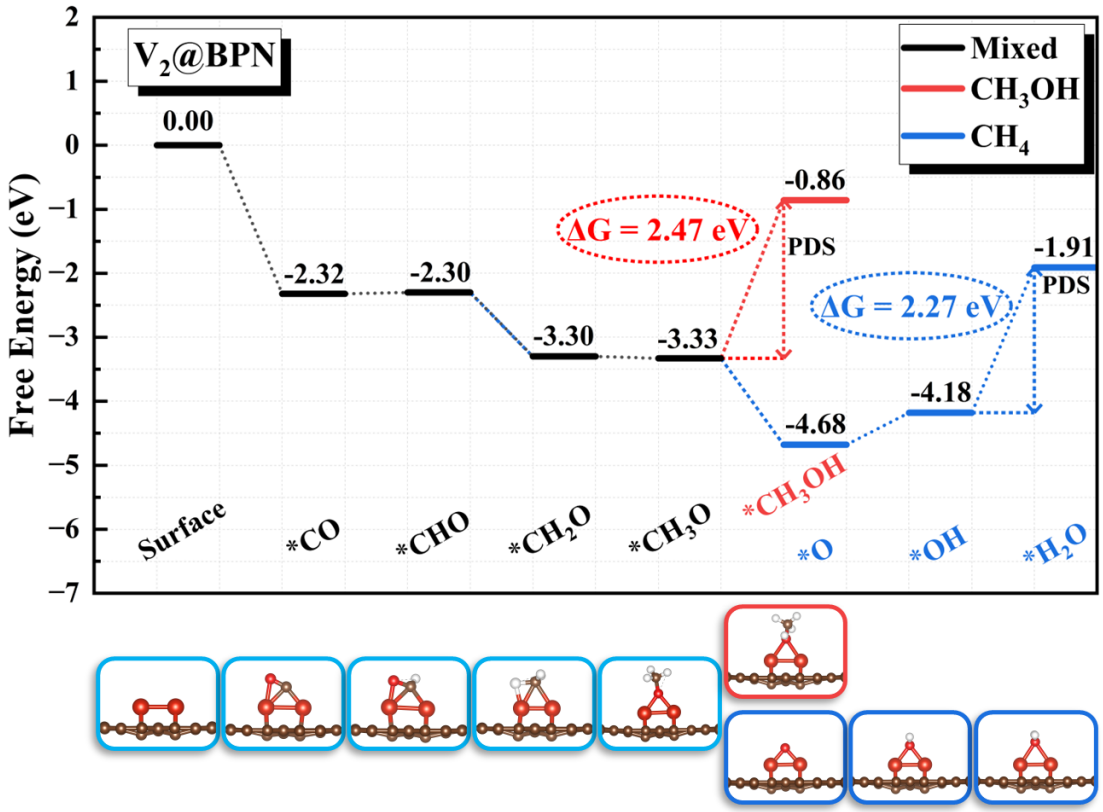

Fig. S14. Free energy diagram of CO reduction to various C_1 on V_2@BPN. The black line represents the common path, the red line represents the CH_3OH path, and the blue line represents the CH_4 path.

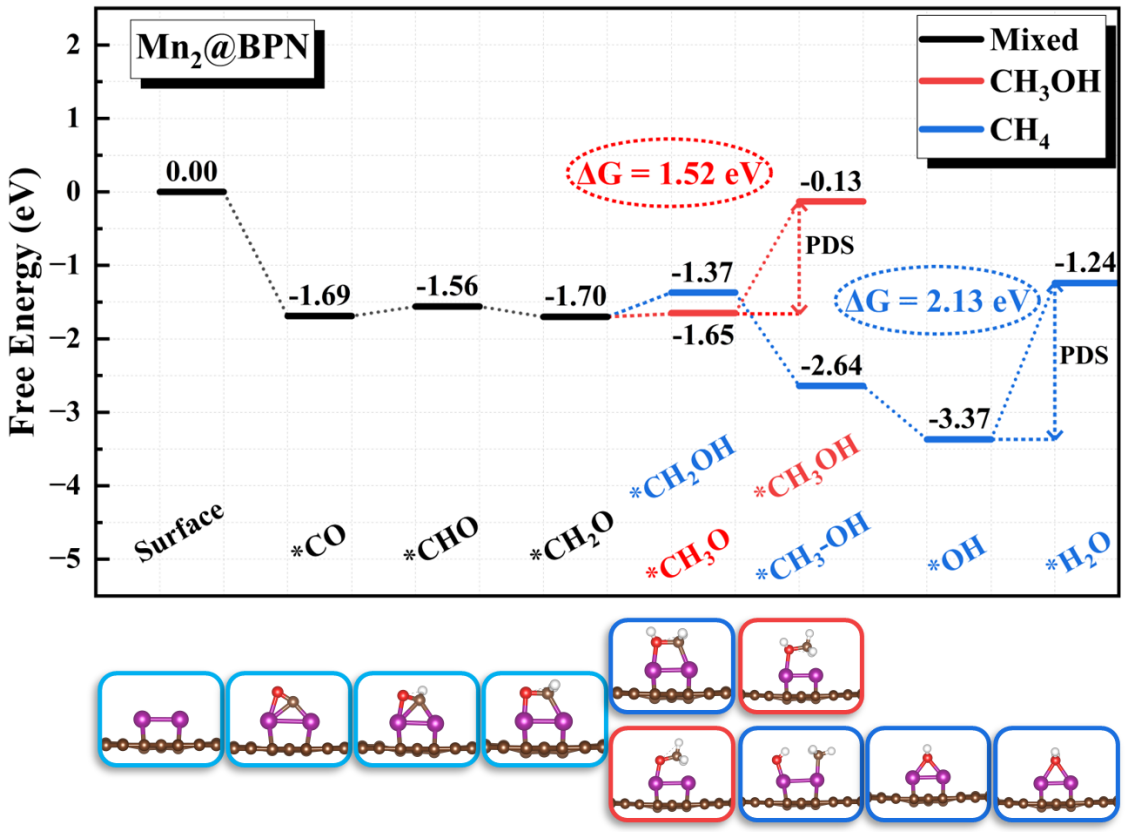

Fig. S15. Free energy diagram of CO reduction to various C_1 on Mn_2@BPN. The black line represents the common path, the red line represents the CH_3OH path, and the blue line represents the CH_4 path.

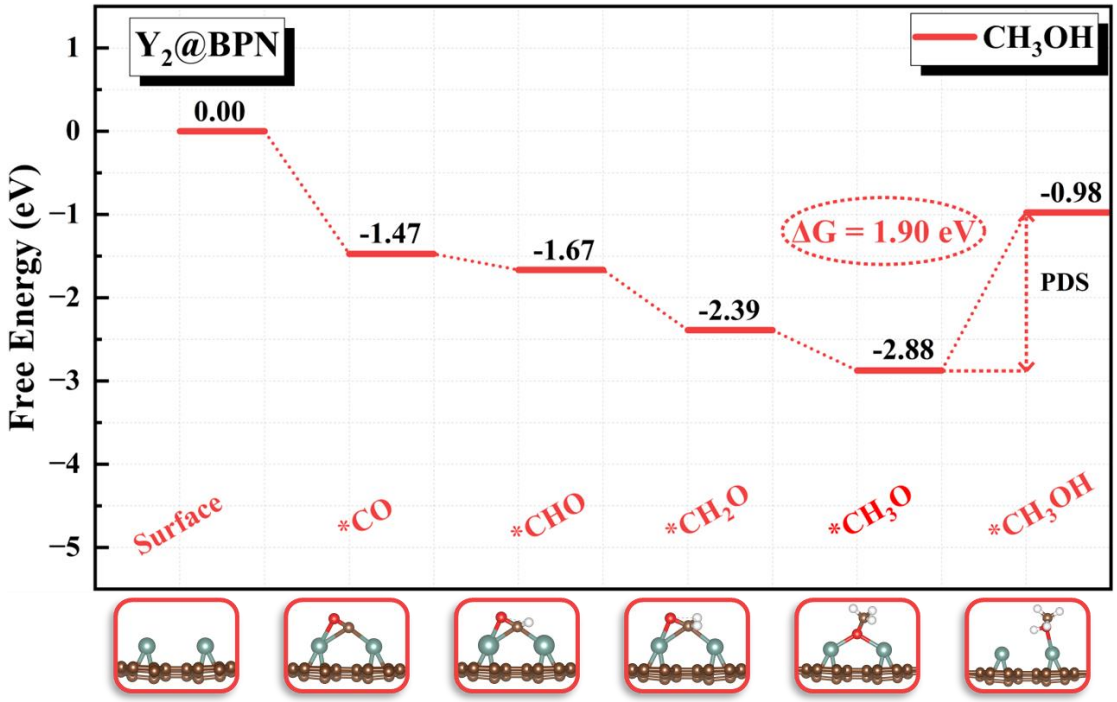

Fig. S16. Free energy diagram of CO reduction to various C_1 on Y_2@BPN. The black line represents the common path, the red line represents the CH_3OH path, and the blue line represents the CH_4 path.

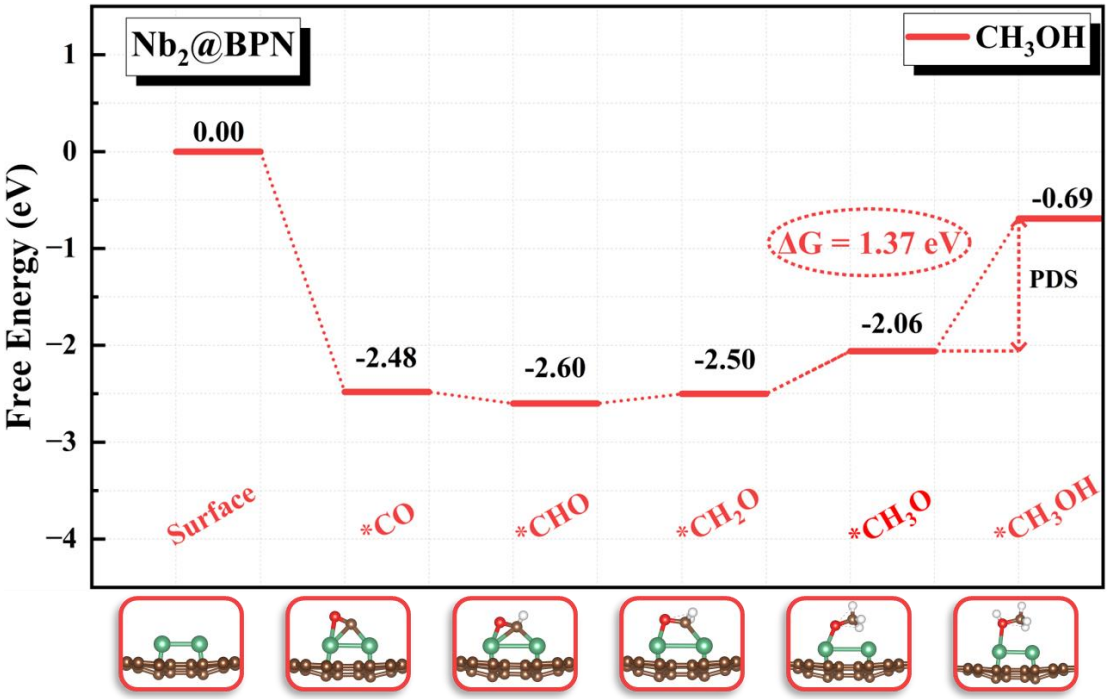

Fig. S17. Free energy diagram of CO reduction to various C_1 on Nb_2@BPN. The black line represents the common path, the red line represents the CH_3OH path, and the blue line represents the CH_4 path.

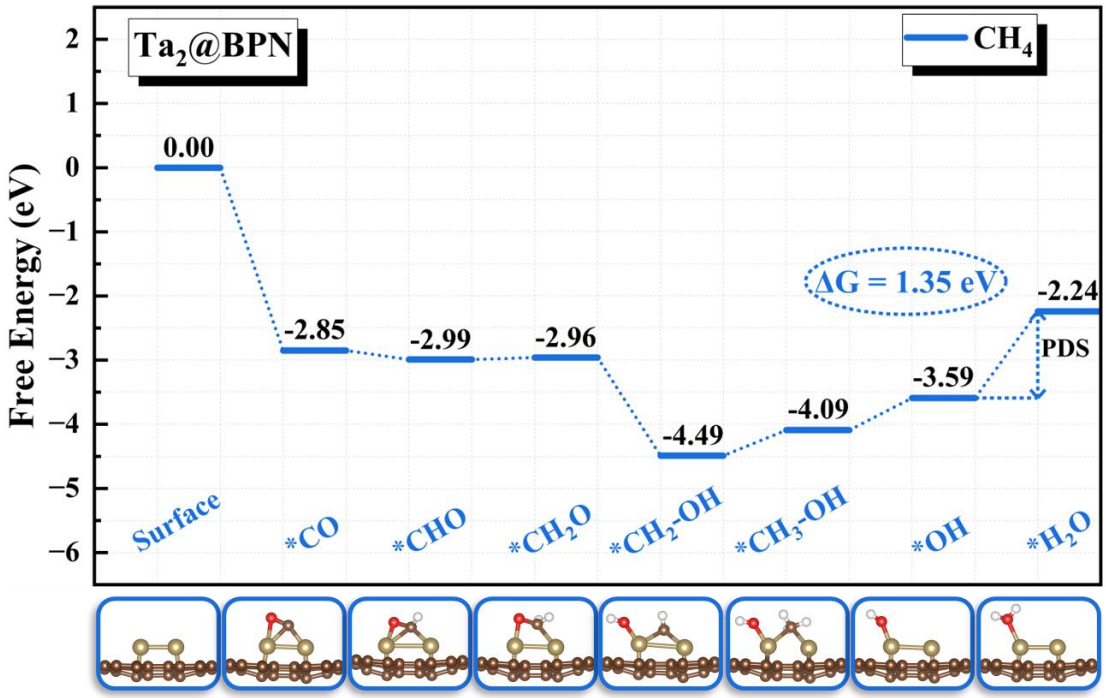

Fig. S18. Free energy diagram of CO reduction to various C_1 on Ta_2@BPN. The black line represents the common path, the red line represents the CH_3OH path, and the blue line represents the CH_4 path.

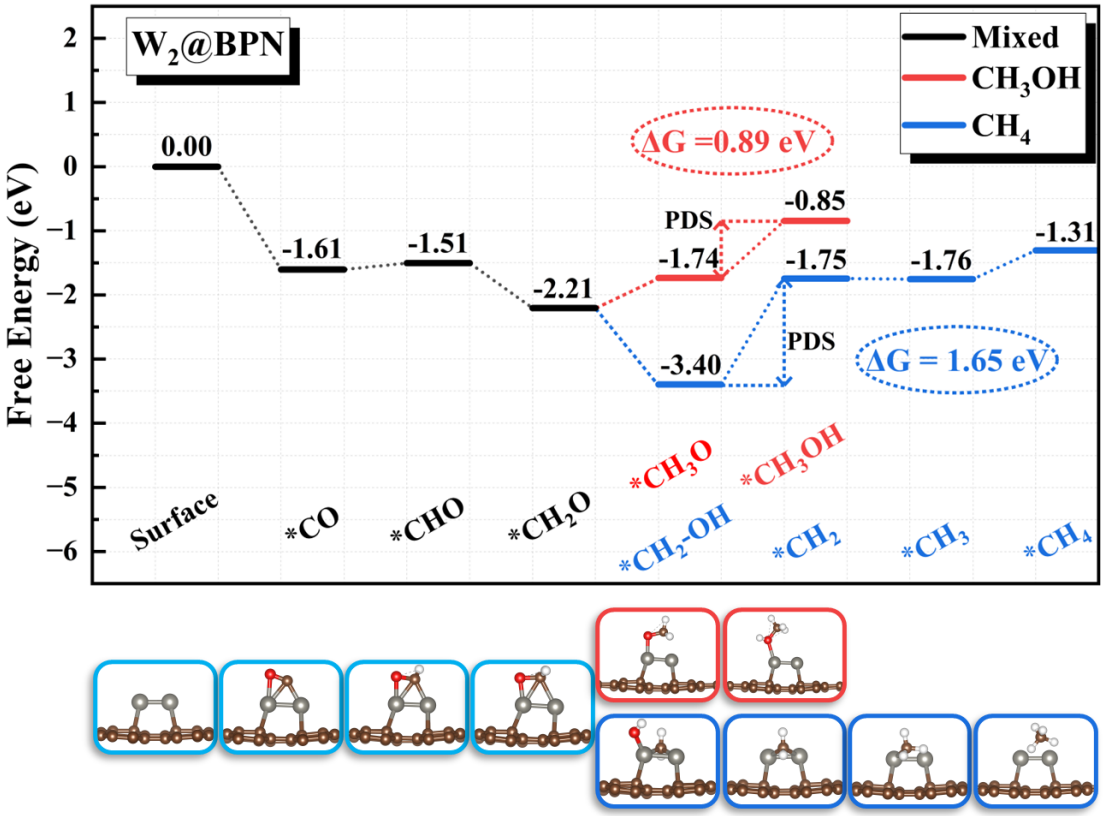

Fig. S19. Free energy diagram of CO reduction to various C_1 on W_2@BPN. The black line represents the common path, the red line represents the CH_3OH path, and the blue line represents the CH_4 path.

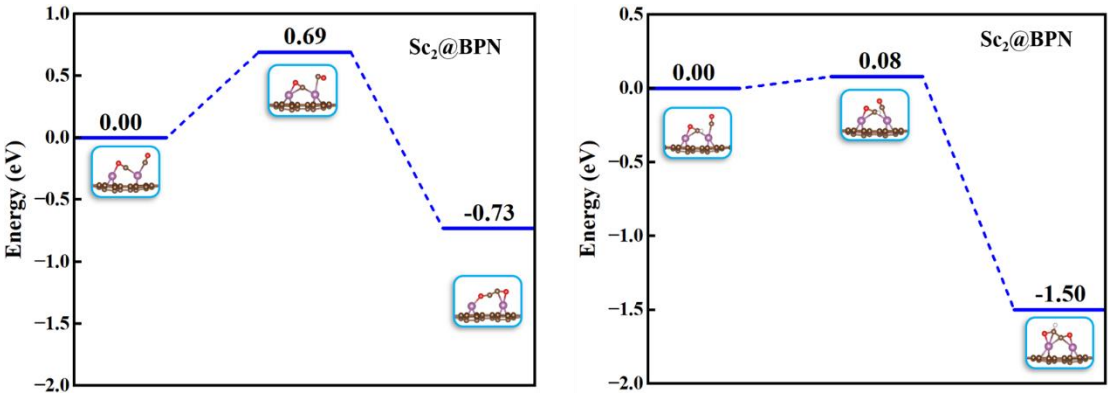

Fig. S20. IS, TS, and FS energy changes involved in the reaction *CO.CO → *COCO and *CHO.CO → *CHOCO for the Sc_2@BPN.

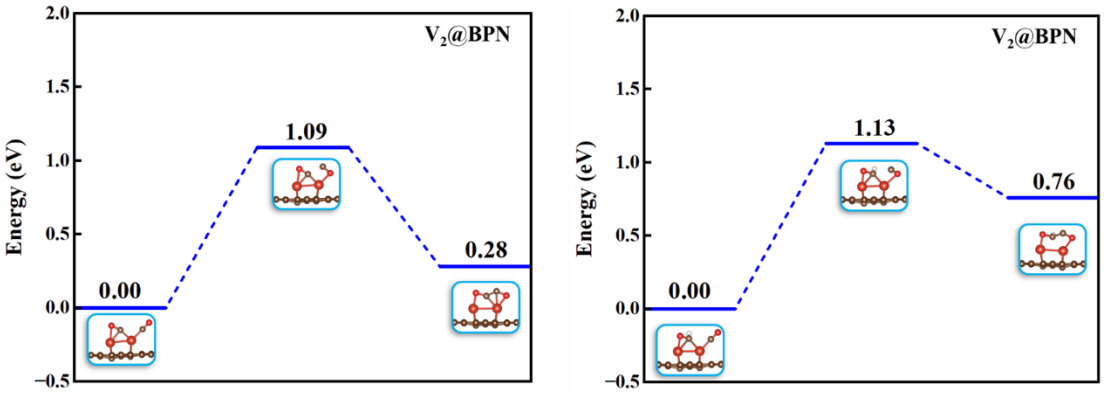

Fig. S21. IS, TS, and FS energy changes involved in the reaction *CO.CO → *COCO and *CHO.CO → *CHOCO for the V_2@BPN.

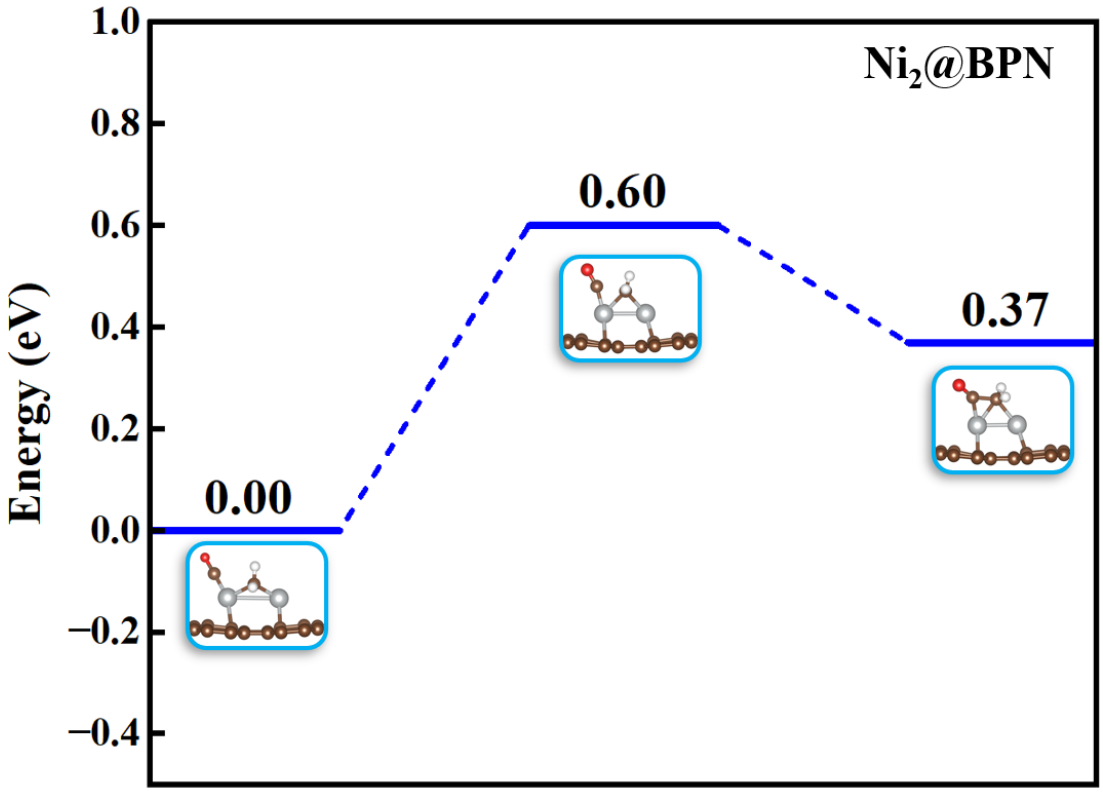

Fig. S22. IS, TS, and FS energy changes involved in the reaction *CH_2.CO → *CH_2CO for the Ni_2@BPN.

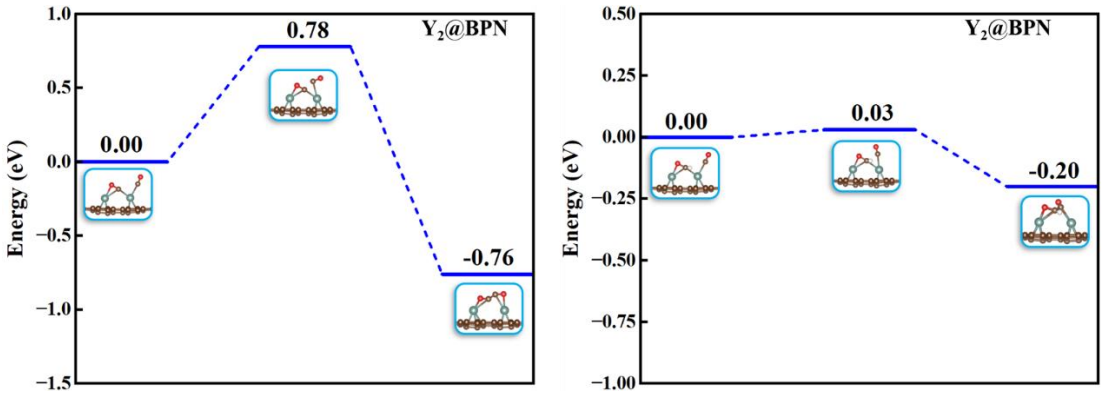

Fig. S23. IS, TS, and FS energy changes involved in the reaction *CO.CO → *COCO and *CHO.CO → *CHOCO for the Y_2@BPN.

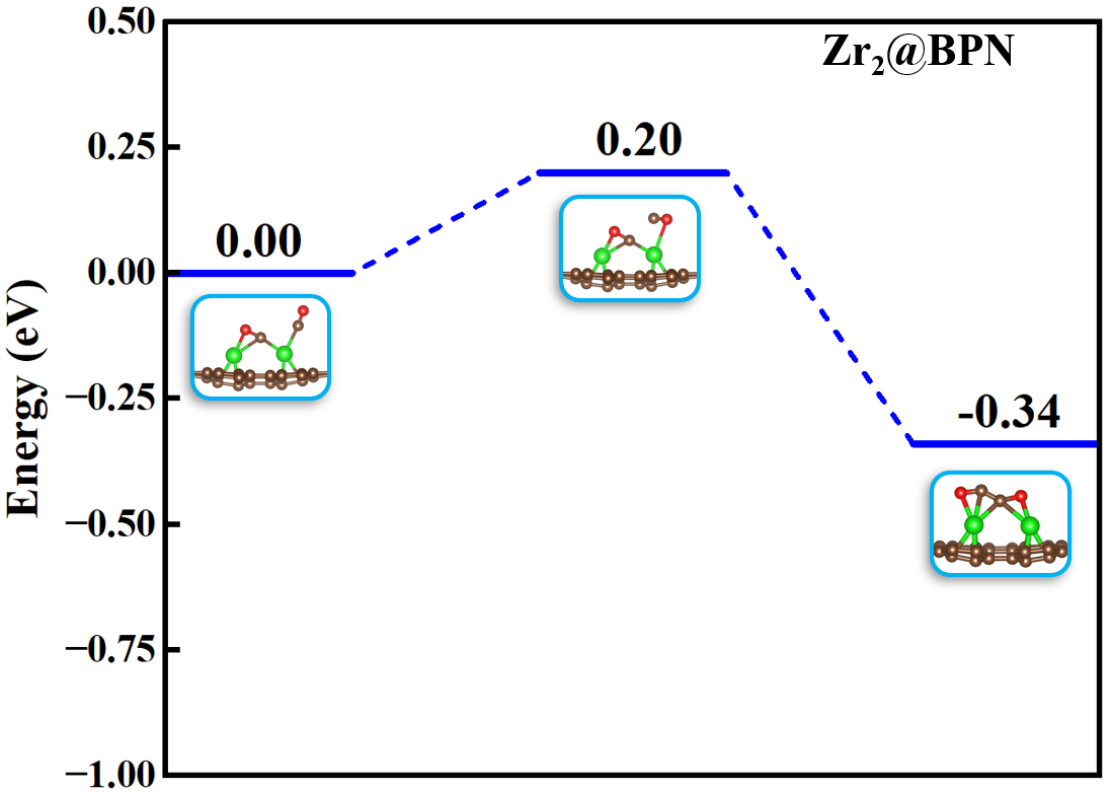

Fig. S24. IS, TS, and FS energy changes involved in the reaction *CO.CO → *COCO for the Zr_2@BPN.

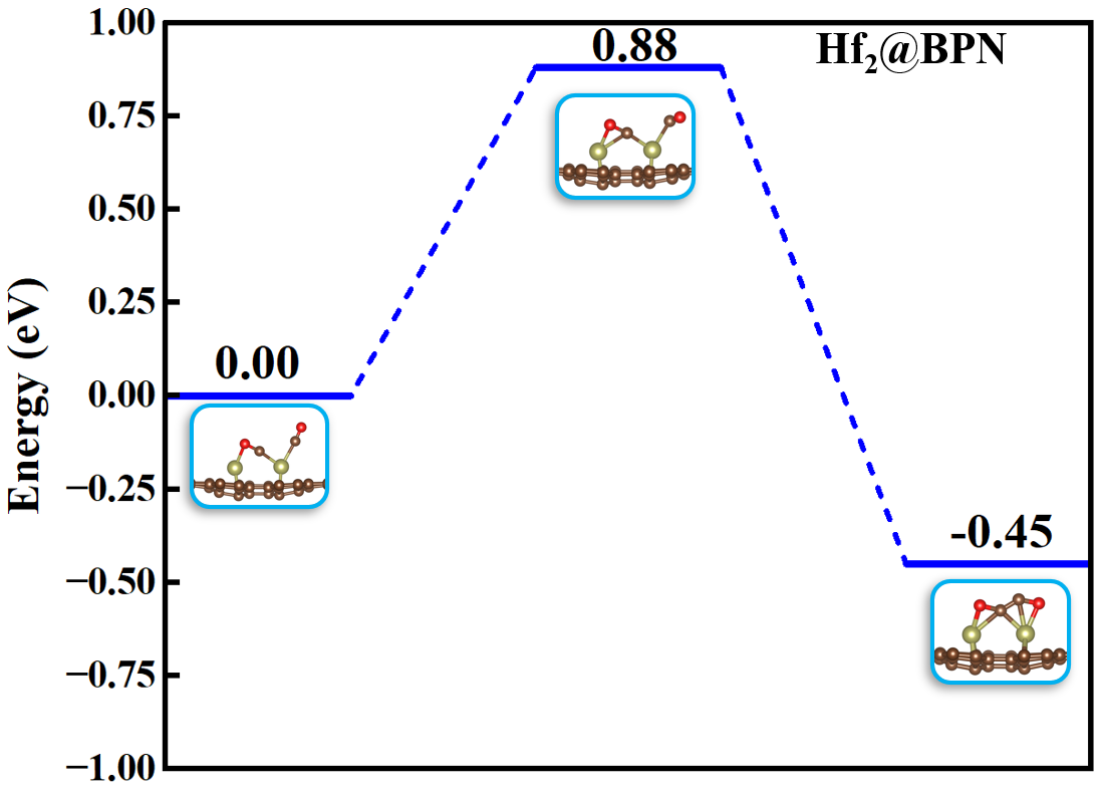

Fig. S25. IS, TS, and FS energy changes involved in the reaction *CO.CO → *COCO for the Hf_2@BPN.

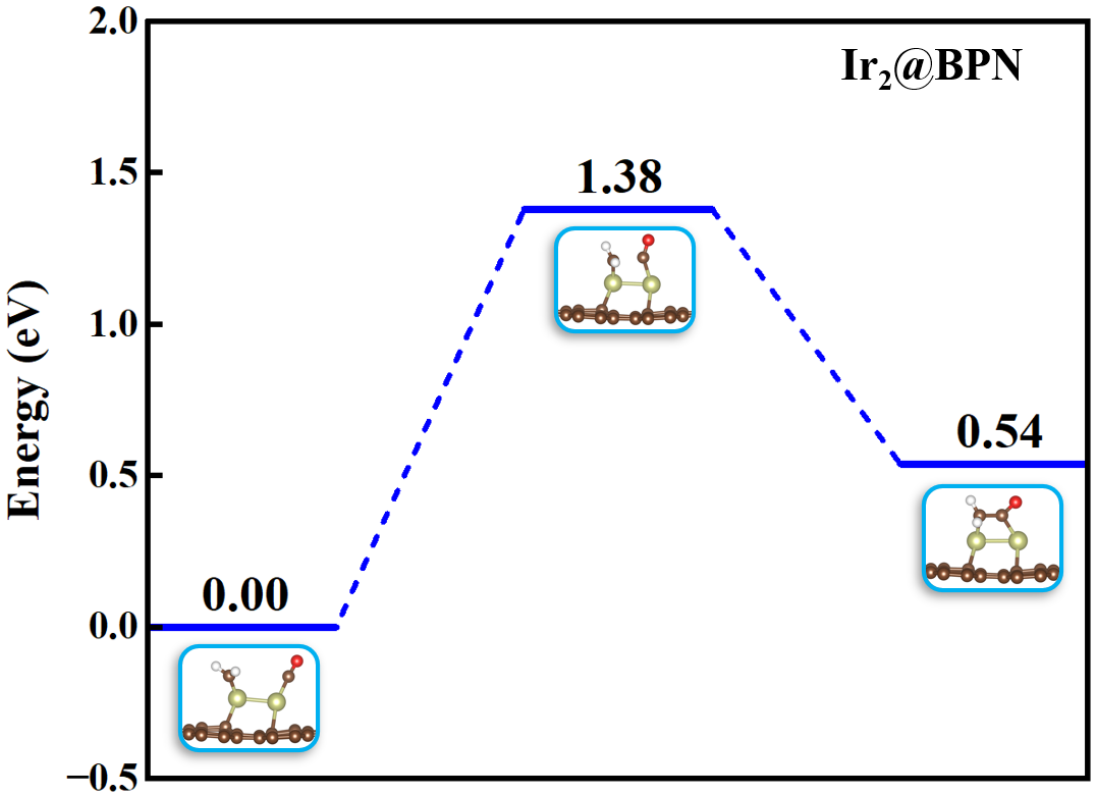

Fig. S26. IS, TS, and FS energy changes involved in the reaction *CH_2.CO → * CH_2CO for the Ir_2@BPN.

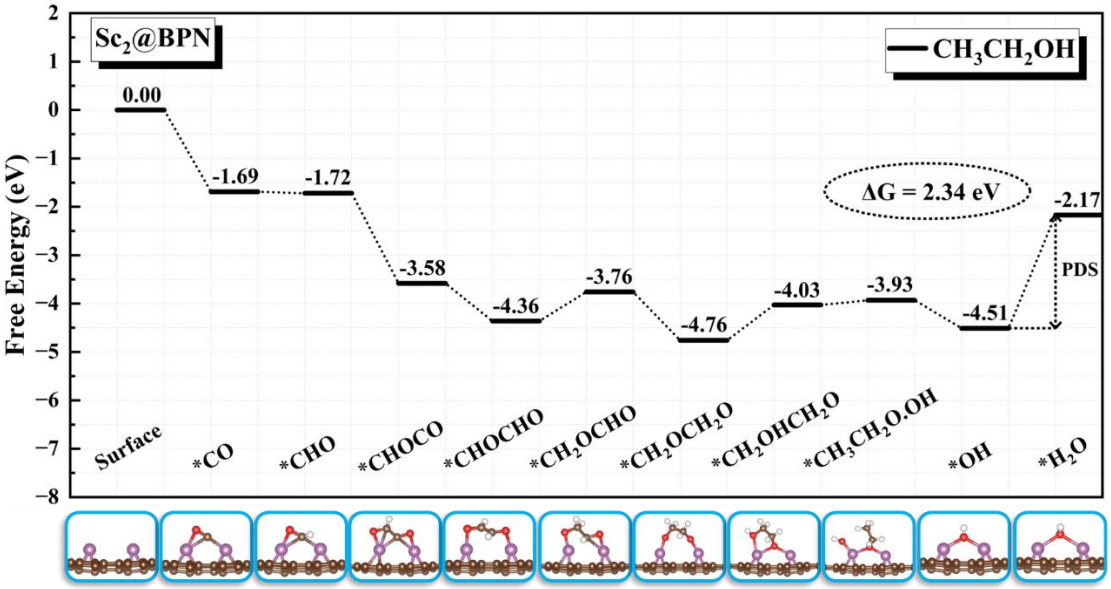

Fig. S27. Free energy diagram of CO reduction to various C_2 on Sc_2@BPN.

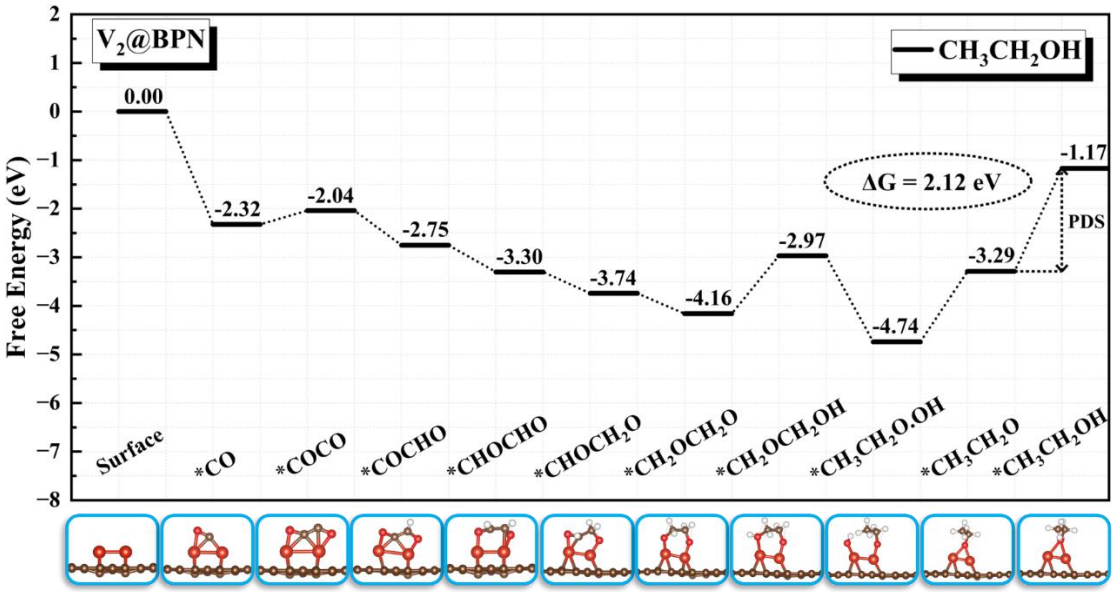

Fig. S28. Free energy diagram of CO reduction to various C_2 on V_2@BPN.

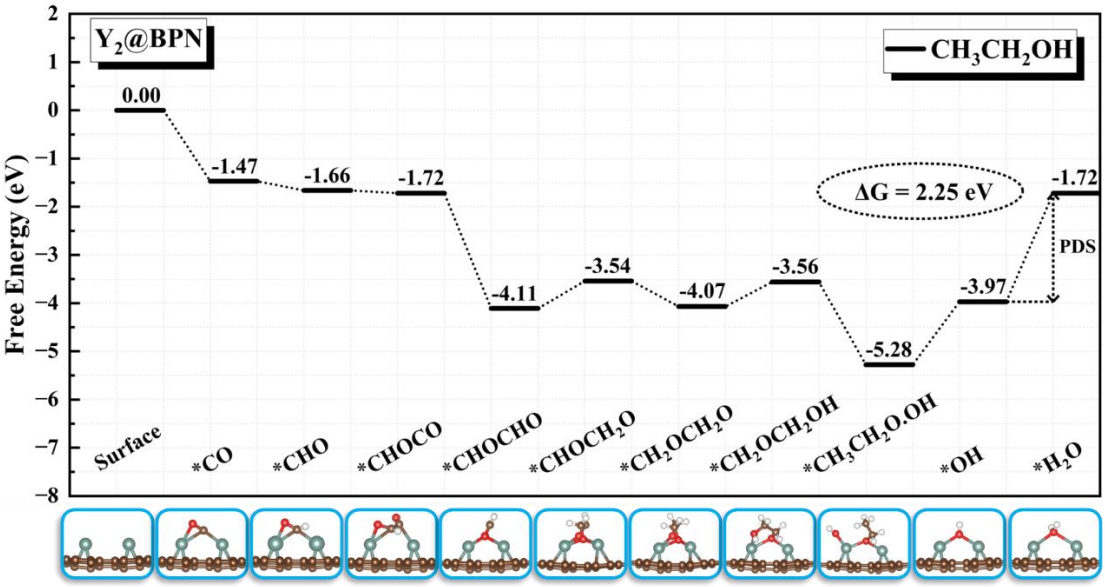

Fig. S29. Free energy diagram of CO reduction to various C_2 on Y_2@BPN.

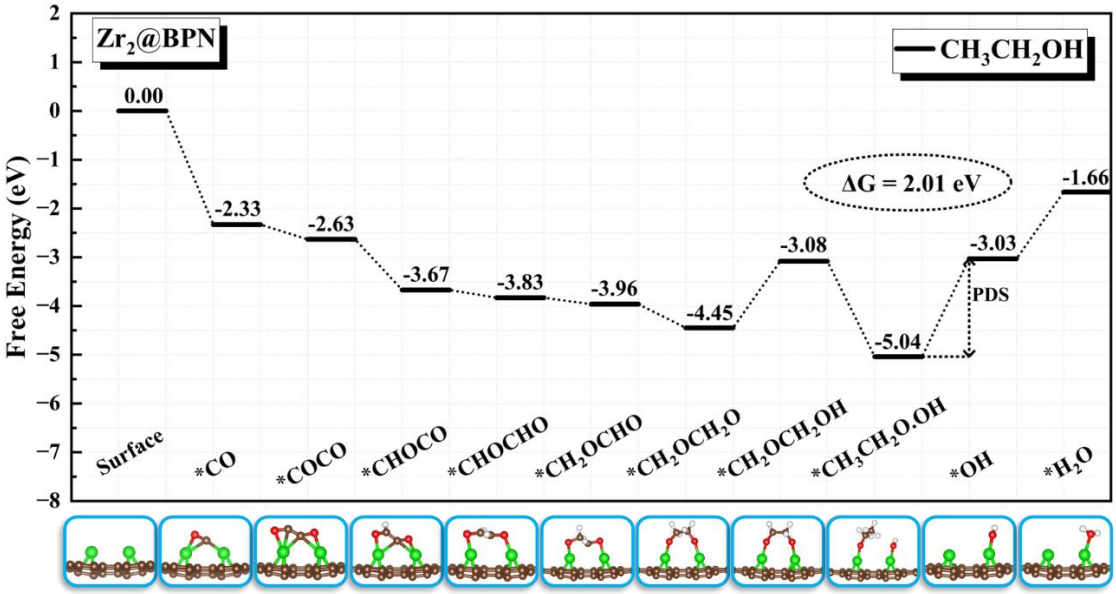

Fig. S30. Free energy diagram of CO reduction to various C_2 on Zr_2@BPN.

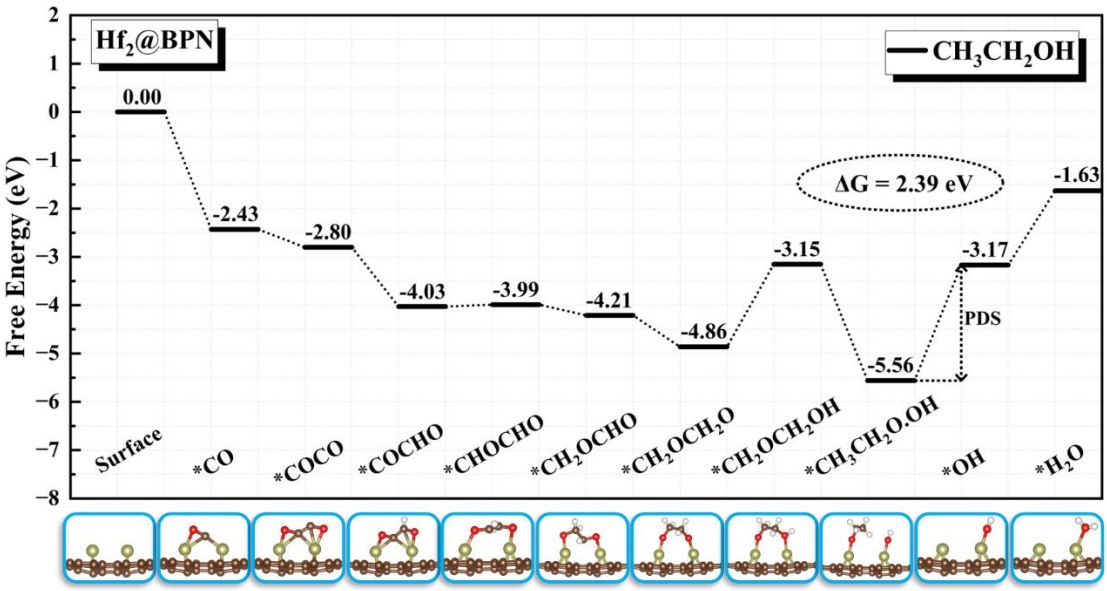

Fig. S31. Free energy diagram of CO reduction to various C_2 on Hf_2@BPN.

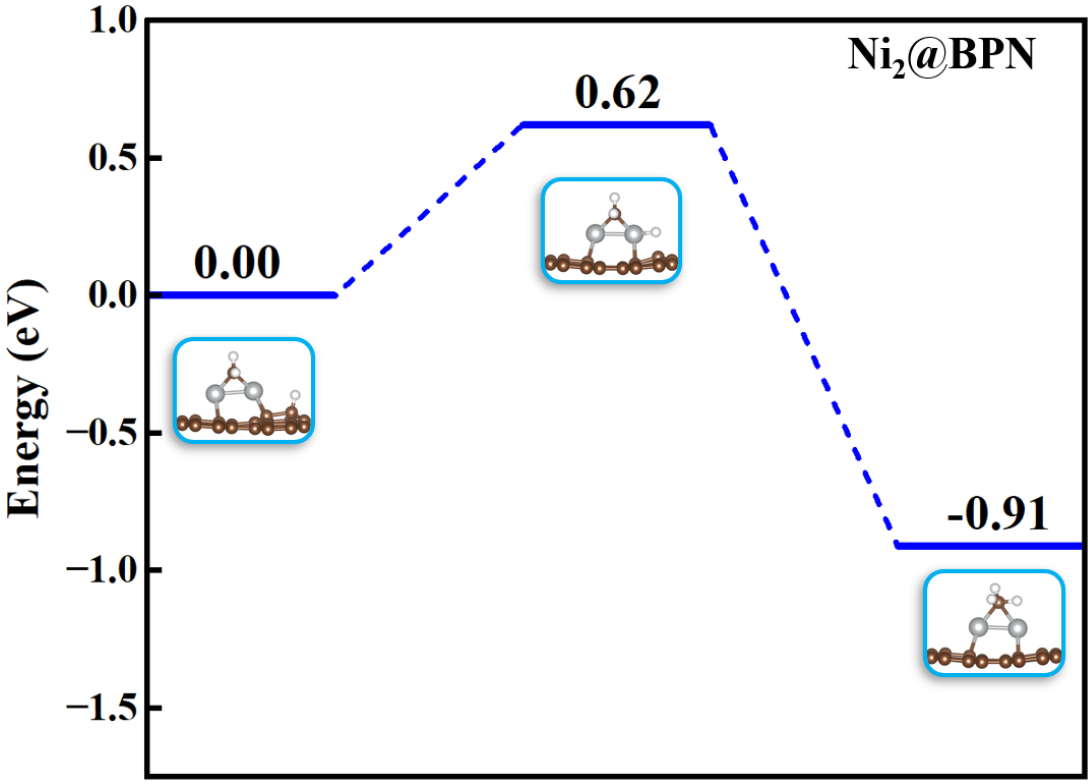

Fig. S32. IS, TS, and FS energy changes involved in the reaction $*CH_2.H \rightarrow *CH_3$ for the Ni_2@BPN.

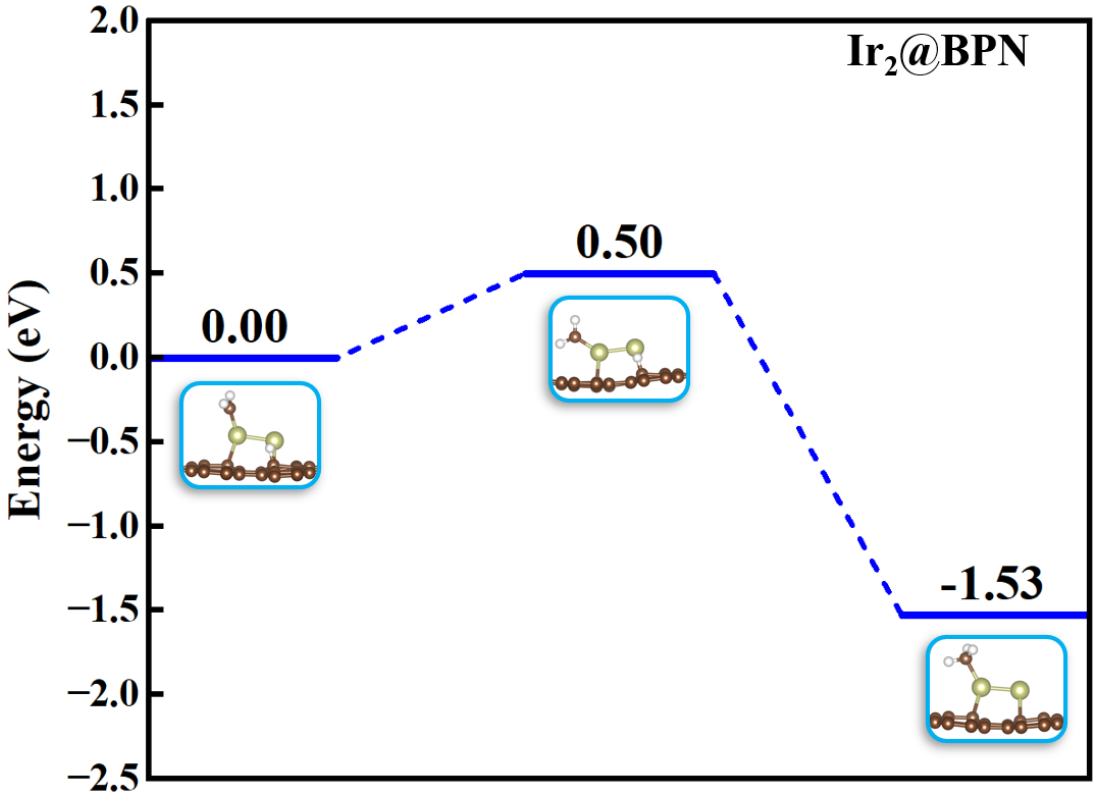

Fig. S33. IS, TS, and FS energy changes involved in the reaction $*CH_2.H \rightarrow *CH_3$ for the Ir_2@BPN.

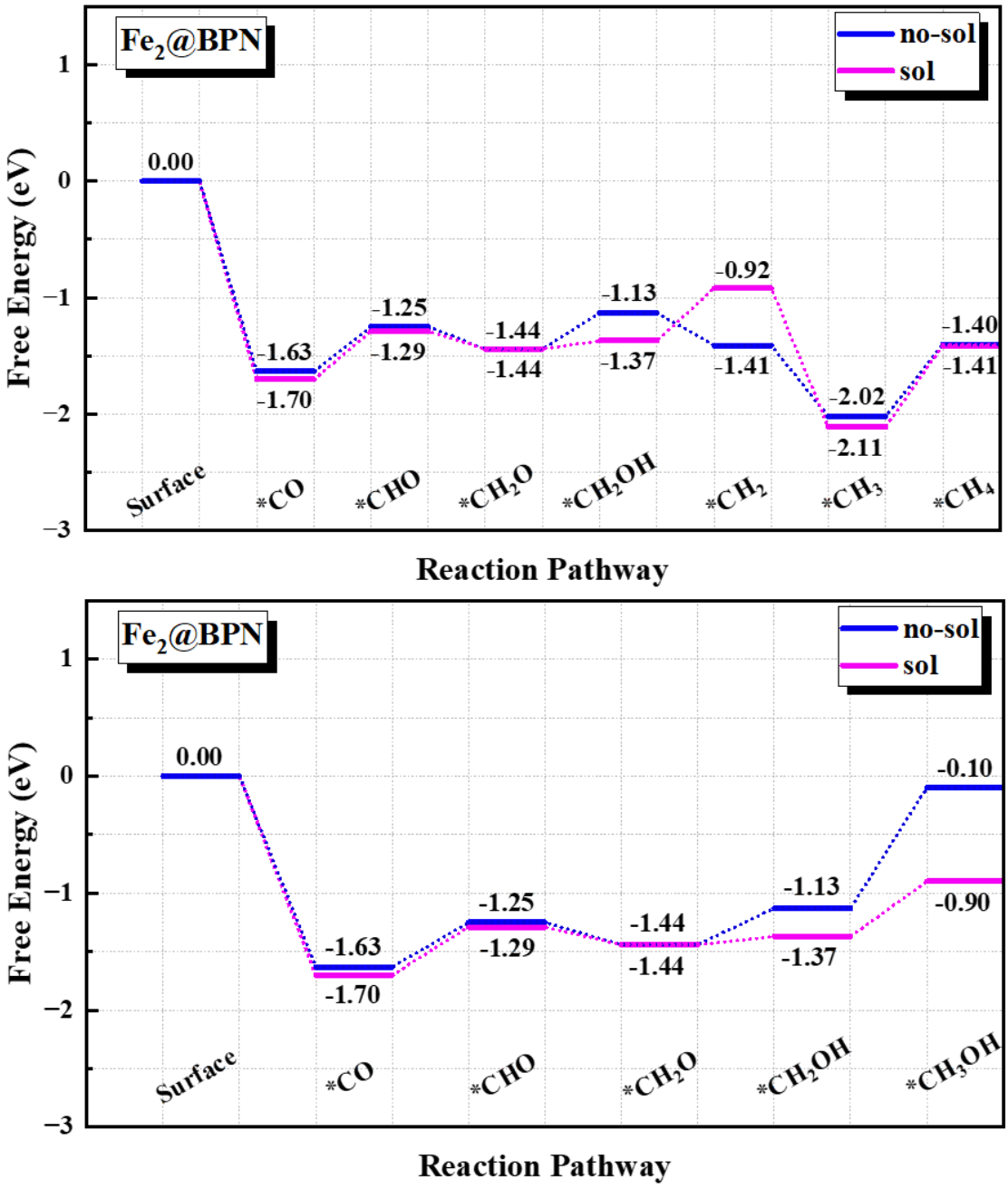

Fig. S34. Free energy diagrams of CORR on Fe_2@BPN without/with solvent effect along the energetically favorable pathway.

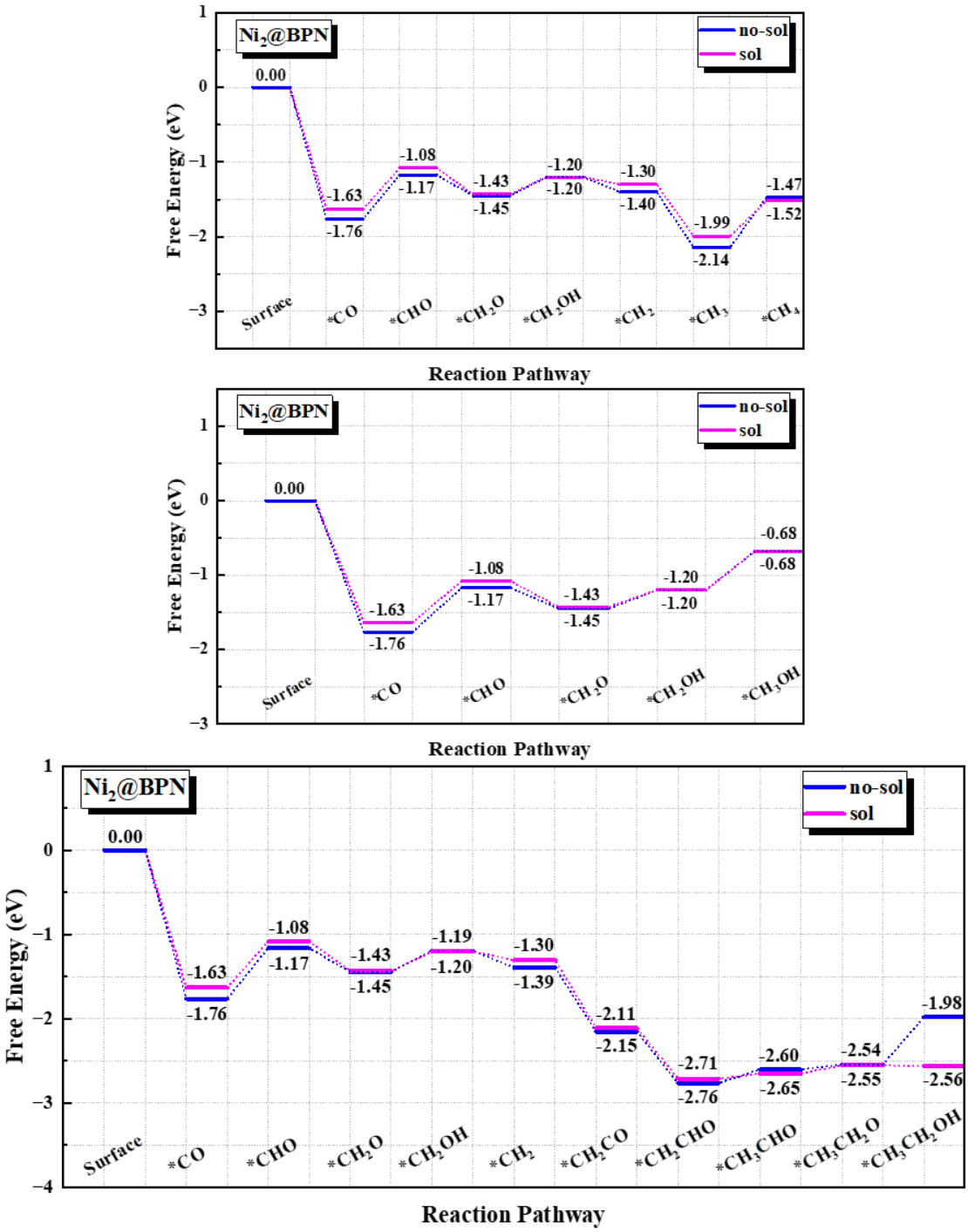

Fig. S35. Free energy diagrams of CORR on Ni_2@BPN without/with solvent effect along the energetically favorable pathway.

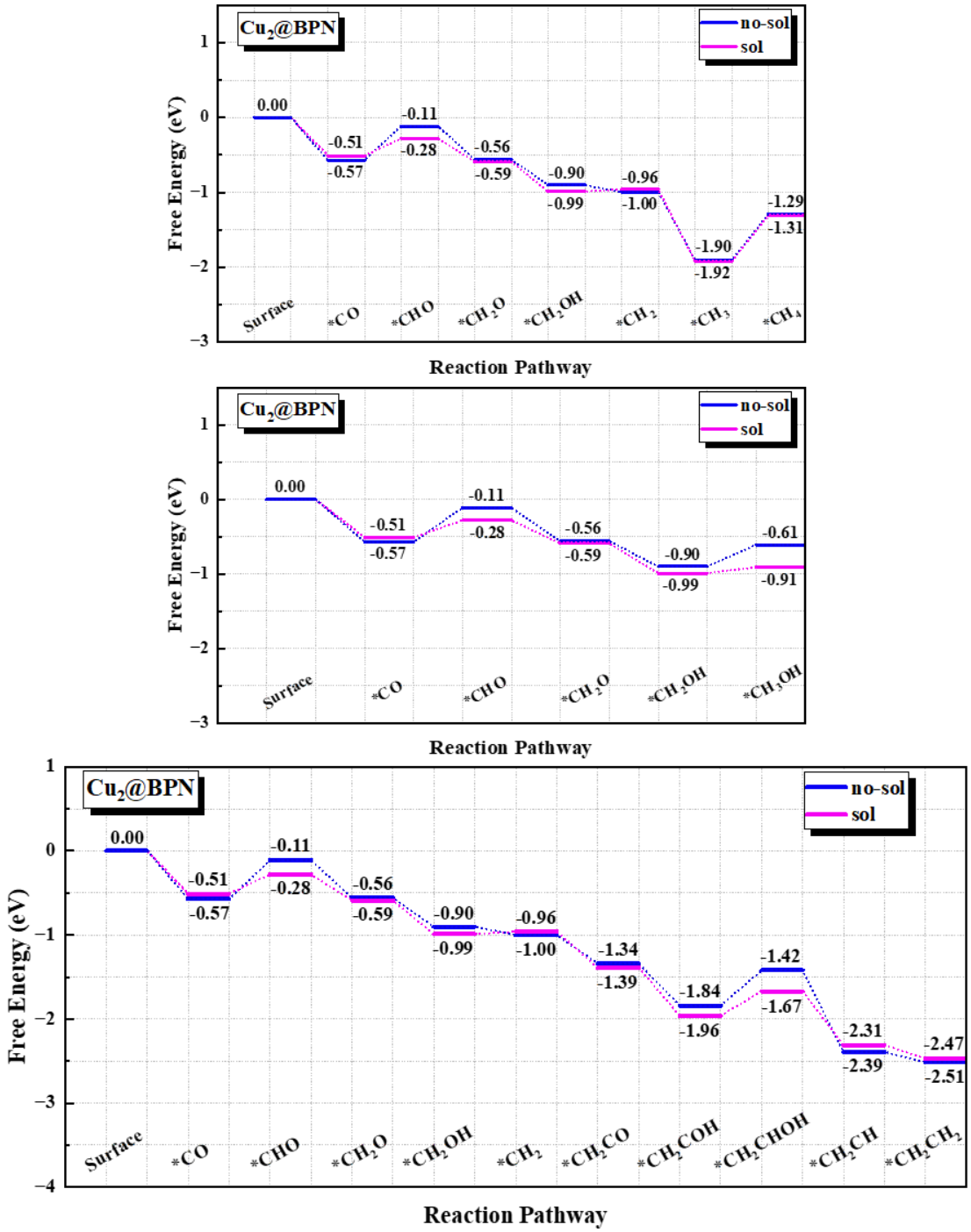

Fig. S36. Free energy diagrams of CORR on Cu_2@BPN without/with solvent effect along the energetically favorable pathway.

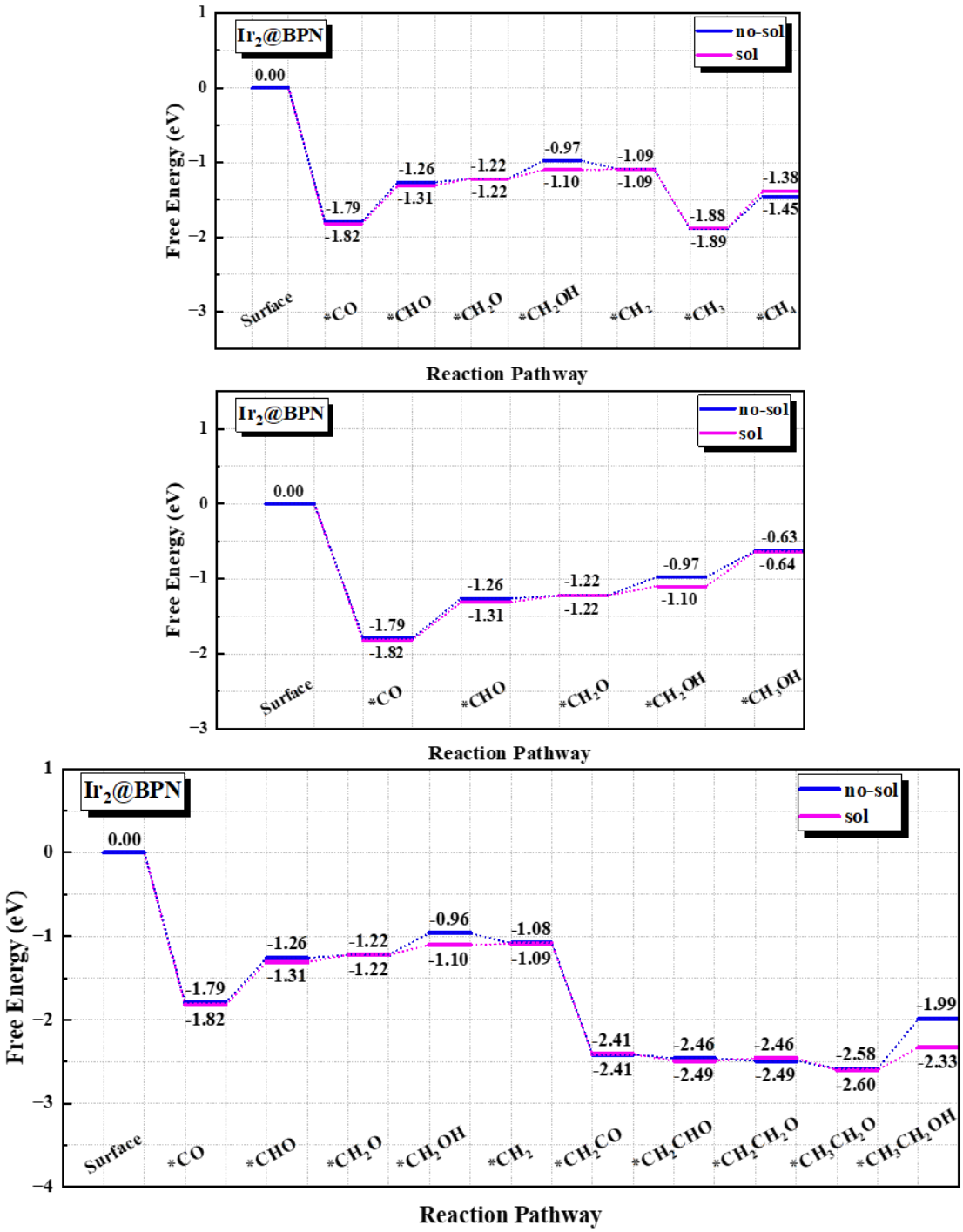

Fig. S37. Free energy diagrams of CORR on Ir_2@BPN without/with solvent effect along the energetically favorable pathway.

Table S1. The most favorable configuration (conf) and relative energy in TM_2@BPN. "/" indicates that this conformation does not exist.

Metal	Conf-I (eV)	Conf-II (eV)	Conf-III(eV)	Conf-IV (eV)	Conf-V (eV)
Sc	Relax to Conf-III	0.66	0	1.18	0.36
Ti	Relax to Conf-III	0	0.03	0.63	1.10
V	0.69	0	/	1.37	/
Cr	0.01	0	Relax to Conf-I	0.95	0.80
Mn	1.39	0	/	0.84	0.78
Fe	0	0.54	Relax to Conf-I	0.69	0.51
Co	0	0.14	/	0.74	0.54
Ni	0	0.38	/	0.83	0.78
Cu	0	0.37	Relax to Conf-I	/	0.03
Zn	0	/	0.01	0.02	0.01
Y	Relax to Conf-III	/	0	1.53	0.40
Zr	Relax to Conf-III	0.82	0	1.31	0.77
Nb	Relax to Conf-III	0.09	0	0.85	Relax to Conf-III
Mo	0	0.20	Relax to Conf-I	0.50	Relax to Conf-I
Ru	0	0.28	/	0.72	0.97
Rh	0.01	0	/	0.76	0.88
Pd	0	0.67	Relax to Conf-I	/	0.56
Ag	0	0.03	0.01	0	0
Cd	0	/	0	0	0
Hf	Relax to Conf-V	0.9	0	1.65	0.66
Ta	0.60	0.28	0	/	/
W	0	0.92	/	Relax to Conf-I	Relax to Conf-I
Re	0	0.50	0.85	1.18	1.11
Os	0	0.66	/	1.18	1.27
Ir	0	0.70	/	1.30	1.04
Pt	0	0.83	Relax to Conf-I	0.74	0.74
Au	0	0.02	/	0	0
Hg	0	/	0	0.01	0.01

Table S2. Binding energy (E_b) of the DACs in the most stable configuration and the cohesion energy (E_{coh}) of the metal atoms in TM_2@BPN.

Metal	E_b (eV)	E_{coh} (eV)
Sc	-7.94	-4.21
Ti	-7.77	-5.40
V	-5.87	-5.35
Cr	-3.06	-4.02
Mn	-3.73	-3.54
Fe	-4.72	-4.84
Co	-5.08	-5.13
Ni	-6.09	-5.01
Cu	-3.19	-3.48
Zn	-0.49	-1.46
Y	-8.20	-4.51
Zr	-10.15	-6.36
Nb	-8.24	-7.48
Mo	-11.54	-9.01
Ru	-9.59	-8.49
Rh	-7.20	-6.53
Pd	-4.43	-4.30
Ag	-2.09	-2.97
Cd	-0.48	-1.07
Hf	-9.39	-6.88
Ta	-9.62	-8.78
W	-9.63	-9.53
Re	-10.08	-9.62
Os	-8.58	-8.91
Ir	-8.22	-8.03
Pt	-7.12	-6.24
Au	-2.70	-3.63
Hg	-0.51	-0.59

Table S3. Structural and electronic properties of TM_2@BPN, including M–M bonds (d_{M-M}), *d* band center (ε_d), magnetic moment (Mag), and charge transfer (CT) from metal dimer to C atoms.

Metal	d_{M-M} (Å)	ε_d (eV)	Mag (μB)	CT (*e*)
Sc	4.01	1.47	1.24	2.25
Ti	2.48	1.05	1.34	1.68
V	2.43	0.40	3.33	1.49
Mn	2.57	-0.48	7.33	1.09
Fe	2.17	-0.95	5.32	0.77
Co	2.17	-1.19	2.68	0.58
Ni	2.36	-1.11	0.62	0.46
Cu	2.35	-2.10	0.00	0.42
Y	4.03	2.06	-1.06	2.55
Zr	3.53	0.85	1.21	2.17
Nb	2.61	0.54	0.93	1.65
Mo	1.73	-0.76	0.75	0.80
Ru	2.28	-1.13	2.99	0.48
Rh	2.65	-1.00	0.30	0.35
Pd	2.67	-1.81	0.00	0.21
Hf	3.30	1.30	0.59	2.15
Ta	2.49	0.86	0.00	1.56
W	2.10	0.12	0.00	0.92
Re	2.14	-0.84	1.39	0.69
Os	2.27	-1.26	3.23	0.46
Ir	2.41	-1.46	1.09	0.19
Pt	2.55	-2.16	0.65	0.05

Table S4. The adsorption energy ΔE (eV) of CO, the Gibbs free energy ΔG (eV) of CO, the bond lengths (Å) of M−C and C-O (d_{M-C} and d_{C-O}), and charge transfer (CT) from metal dimer to CO.

Metal	ΔE_{*CO} (eV)	ΔG_{*CO} (eV)	d_{M-C} (Å)	d_{C-O} (Å)	CT (*e*)
Sc	-2.31	-1.69	2.23	1.25	-0.95
Ti	-2.68	-2.05	2.03	1.26	-1.07
V	-2.92	-2.32	1.97	1.26	-0.95
Mn	-2.34	-1.69	1.95	1.24	-0.82
Fe	-2.22	-1.63	1.88	1.23	-0.69
Co	-2.65	-2.00	1.91	1.19	-0.42
Ni	-2.34	-1.76	1.88	1.22	-0.52
Cu	-1.14	-0.57	1.93	1.19	-0.36
Y	-2.09	-1.47	2.40	1.24	-1.08
Zr	-2.96	-2.33	2.25	1.27	-1.12
Nb	-3.12	-2.48	2.08	1.28	-1.12
Mo	-1.13	-0.96	2.25	1.18	-0.44
Ru	-2.43	-1.80	2.01	1.21	-0.50
Rh	-2.58	-2.05	2.04	1.19	-0.35
Pd	-1.88	-1.27	2.00	1.18	-0.21
Hf	-3.03	-2.43	2.20	1.30	-1.21
Ta	-3.51	-2.85	2.05	1.31	-1.16
W	-2.24	-1.61	2.05	1.28	-0.85
Re	-2.25	-1.59	1.94	1.18	-0.38
Os	-2.50	-1.83	1.87	1.18	-0.28
Ir	-2.42	-1.79	1.98	1.21	-0.41
Pt	-2.29	-1.64	1.86	1.17	-0.12

Table S5. The values of the free energy change (ΔG/eV) at each step involved in Sc_2@BPN.

Reaction process	ΔG
$*CO + H^+ + e^- \rightarrow *CHO$	–0.03
$*CO + H^+ + e^- \rightarrow *COH$	1.55
$*CHO + H^+ + e^- \rightarrow *CH_2O$	–0.92
$*CHO + H^+ + e^- \rightarrow *CHOH$	0.61
$*CH_2O + H^+ + e^- \rightarrow *CH_3O$	–0.54
$*CH_2O + H^+ + e^- \rightarrow *CH_2OH$	1.11
$*CH_3O + H^+ + e^- \rightarrow *O + CH_4$ (g)	–1.76
$*CH_3O + H^+ + e^- \rightarrow *CH_3OH$	2.34
$*O + H^+ + e^- \rightarrow *OH$	0.57
$*OH + H^+ + e^- \rightarrow *H_2O$ (l)	2.39

Table S6. The values of the free energy change (ΔG/eV) at each step involved in Ti_2@BPN.

Reaction process	ΔG
$*CO + H^+ + e^- \rightarrow *CHO$	0.03
$*CO + H^+ + e^- \rightarrow *COH$	1.52
$*CHO + H^+ + e^- \rightarrow *CH_2O$	–0.41
$*CHO + H^+ + e^- \rightarrow *CHOH$	0.87
$*CH_2O + H^+ + e^- \rightarrow *CH_3O$	–0.60
$*CH_2O + H^+ + e^- \rightarrow *CH_2OH$	0.62
$*CH_3O + H^+ + e^- \rightarrow *O + CH_4$ (g)	–1.43
$*CH_3O + H^+ + e^- \rightarrow *CH_3OH$	2.17
$*O + H^+ + e^- \rightarrow *OH$	0.32
$*OH + H^+ + e^- \rightarrow *H_2O$ (l)	2.17

Table S7. The values of the free energy change (ΔG/eV) at each step involved in V_2@BPN.

Reaction process	ΔG
$*CO + H^+ + e^- \rightarrow *CHO$	0.02
$*CO + H^+ + e^- \rightarrow *COH$	1.48
$*CHO + H^+ + e^- \rightarrow *CH_2O$	–1.00
$*CHO + H^+ + e^- \rightarrow *CHOH$	0.62
$*CH_2O + H^+ + e^- \rightarrow *CH_3O$	–0.03
$*CH_2O + H^+ + e^- \rightarrow *CH_2OH$	1.32
$*CH_3O + H^+ + e^- \rightarrow *O + CH_4$ (g)	–1.35
$*CH_3O + H^+ + e^- \rightarrow *CH_3OH$	2.47
$*O + H^+ + e^- \rightarrow *OH$	0.50
$*OH + H^+ + e^- \rightarrow *H_2O$ (l)	2.27

Table S8. The values of the free energy change (ΔG/eV) at each step involved in Mn_2@BPN.

Reaction process	ΔG
$*CO + H^+ + e^- \rightarrow *CHO$	0.13
$*CO + H^+ + e^- \rightarrow *COH$	1.08
$*CHO + H^+ + e^- \rightarrow *CH_2O$	–0.14
$*CHO + H^+ + e^- \rightarrow *CHOH$	0.77
$*CH_2O + H^+ + e^- \rightarrow *CH_3O$	0.05
$*CH_2O + H^+ + e^- \rightarrow *CH_2OH$	0.33
$*CH_3O + H^+ + e^- \rightarrow *CH_3OH$	1.52
$*CH_2OH + H^+ + e^- \rightarrow *CH_3\text{-}OH$	–1.27
$*CH_2OH + H^+ + e^- \rightarrow *CH_2 + H_2O(l)$	–0.19
$*CH_3\text{-}OH + H^+ + e^- \rightarrow *OH + CH_4\,(g)$	–0.73
$*CH_3\text{-}OH + H^+ + e^- \rightarrow *CH_3 + H_2O(l)$	0.27
$*OH + H^+ + e^- \rightarrow *H_2O$	2.13

Table S9. The values of the free energy change (ΔG/eV) at each step involved in Fe_2@BPN.

Reaction process	ΔG
$*CO + H^+ + e^- \rightarrow *CHO$	0.38
$*CO + H^+ + e^- \rightarrow *COH$	1.37
$*CHO + H^+ + e^- \rightarrow *CH_2O$	–0.19
$*CHO + H^+ + e^- \rightarrow *CHOH$	0.63
$*CH_2O + H^+ + e^- \rightarrow *CH_3O$	0.21
$*CH_2O + H^+ + e^- \rightarrow *CH_2OH$	0.31
$*CH_3O + H^+ + e^- \rightarrow *CH_3OH$	1.13
$*CH_2OH + H^+ + e^- \rightarrow *CH_3OH$	1.02
$*CH_2OH + H^+ + e^- \rightarrow *CH_2 + H_2O$ (l)	–0.28
$*CH_2 + H^+ + e^- \rightarrow *CH_3$	–0.61
$*CH_3 + H^+ + e^- \rightarrow *CH_4$(g)	0.62

Table S10. The values of the free energy change (ΔG/eV) at each step involved in Ni_2@BPN.

Reaction process	ΔG
$*CO + H^+ + e^- \rightarrow *CHO$	0.59
$*CO + H^+ + e^- \rightarrow *COH$	1.95
$*CHO + H^+ + e^- \rightarrow *CH_2O$	–0.28
$*CHO + H^+ + e^- \rightarrow *CHOH$	0.50
$*CH_2O + H^+ + e^- \rightarrow *CH_3O$	–0.23
$*CH_2O + H^+ + e^- \rightarrow *CH_2OH$	0.25
$*CH_3O + H^+ + e^- \rightarrow *CH_3OH$	1.00
$*CH_2OH + H^+ + e^- \rightarrow *CH_3OH$	0.51
$*CH_2OH + H^+ + e^- \rightarrow *CH_2 + H_2O$ (l)	–0.20
$*CH_2 + H^+ + e^- \rightarrow *CH_3$	–0.74
$*CH_3 + H^+ + e^- \rightarrow * CH_4$(g)	0.67

Table S11. The values of the free energy change (ΔG/eV) at each step involved in Cu_2@BPN.

Reaction process	ΔG
$*CO + H^+ + e^- \rightarrow *CHO$	0.46
$*CO + H^+ + e^- \rightarrow *COH$	1.14
$*CHO + H^+ + e^- \rightarrow *CH_2O$	–0.45
$*CHO + H^+ + e^- \rightarrow *CHOH$	0.03
$*CH_2O + H^+ + e^- \rightarrow *CH_3O$	–0.30
$*CH_2O + H^+ + e^- \rightarrow *CH_2OH$	–0.34
$*CH_3O + H^+ + e^- \rightarrow *CH_3OH$	0.33
$*CH_2OH + H^+ + e^- \rightarrow *CH_3OH$	0.29
$*CH_2OH + H^+ + e^- \rightarrow *CH_2 + H_2O$ (l)	–0.10
$*CH_2 + H^+ + e^- \rightarrow *CH_3$	–0.90
$*CH_3 + H^+ + e^- \rightarrow *CH_4$	0.61

Table S12. The values of the free energy change (ΔG/eV) at each step involved in Y_2@BPN.

Reaction process	ΔG
$*CO + H^+ + e^- \rightarrow *CHO$	–0.19
$*CO + H^+ + e^- \rightarrow *COH$	1.63
$*CHO + H^+ + e^- \rightarrow *CH_2O$	–0.72
$*CHO + H^+ + e^- \rightarrow *CHOH$	0.78
$*CH_2O + H^+ + e^- \rightarrow *CH_3O$	–0.48
$*CH_2O + H^+ + e^- \rightarrow *CH_2OH$	0.98
$*CH_3O + H^+ + e^- \rightarrow *CH_3OH$	1.90

Table S13. The values of the free energy change (ΔG/eV) at each step involved in Nb_2@BPN.

Reaction process	ΔG
$*CO + H^+ + e^- \rightarrow *CHO$	–0.12
$*CO + H^+ + e^- \rightarrow *COH$	0.97
$*CHO + H^+ + e^- \rightarrow *CH_2O$	0.10
$*CHO + H^+ + e^- \rightarrow *CHOH$	1.11
$*CH_2O + H^+ + e^- \rightarrow *CH_3O$	0.44
$*CH_2O + H^+ + e^- \rightarrow *CH_2OH$	1.29
$*CH_3O + H^+ + e^- \rightarrow *CH_3OH$	1.37

Table S14. The values of the free energy change (ΔG/eV) at each step involved in Ta_2@BPN.

Reaction process	ΔG
$*CO + H^+ + e^- \rightarrow *CHO$	–0.14
$*CO + H^+ + e^- \rightarrow *COH$	1.04
$*CHO + H^+ + e^- \rightarrow *CH_2O$	0.03
$*CHO + H^+ + e^- \rightarrow *CHOH$	1.26
$*CH_2O + H^+ + e^- \rightarrow *CH_3\text{-}O$	–1.22
$*CH_2O + H^+ + e^- \rightarrow *CH_2\text{-}OH$	–1.53
$*CH_2\text{-}OH + H^+ + e^- \rightarrow *CH_3\text{-}OH$	0.40
$*CH_2\text{-}OH + H^+ + e^- \rightarrow *CH_2\text{-}H_2O$ (l)	1.92
$*CH_3\text{-}OH + H^+ + e^- \rightarrow *OH + CH_4$(g)	0.50
$*CH_3\text{-}OH + H^+ + e^- \rightarrow *CH_3 + H_2O$ (l)	2.09
$*OH + H^+ + e^- \rightarrow *H_2O$ (l)	1.35

Table S15. The values of the free energy change (ΔG/eV) at each step involved in W_2@BPN.

Reaction process	ΔG
$*CO + H^+ + e^- \rightarrow *CHO$	0.10
$*CO + H^+ + e^- \rightarrow *COH$	1.13
$*CHO + H^+ + e^- \rightarrow *CH_2O$	–0.70
$*CHO + H^+ + e^- \rightarrow *CHOH$	0.96
$*CH_2O + H^+ + e^- \rightarrow *CH_3O$	0.47
$*CH_2O + H^+ + e^- \rightarrow *CH_2\text{-}OH$	–1.19
$*CH_3O + H^+ + e^- \rightarrow *CH_3OH$	0.89
$*CH_2\text{-}OH + H^+ + e^- \rightarrow *CH_2\text{-}H_2O$ (l)	1.65
$*CH_2 + H^+ + e^- \rightarrow *CH_3$	–0.01
$*CH_3 + H^+ + e^- \rightarrow *CH_4$	0.45

Table S16. The values of the free energy change (ΔG/eV) at each step involved in Ir_2@BPN.

Reaction process	ΔG
$*CO + H^+ + e^- \rightarrow *CHO$	0.53
$*CO + H^+ + e^- \rightarrow *COH$	0.67
$*CHO + H^+ + e^- \rightarrow *CH_2O$	0.04
$*CHO + H^+ + e^- \rightarrow *CHOH$	0.17
$*CH_2O + H^+ + e^- \rightarrow *CH_3O$	–0.11
$*CH_2O + H^+ + e^- \rightarrow *CH_2OH$	0.25
$*CH_3O + H^+ + e^- \rightarrow *CH_3OH$	0.70
$*CH_2OH + H^+ + e^- \rightarrow *CH_2\text{-}H_2O$ (l)	–0.12
$*CH_2 + H^+ + e^- \rightarrow *CH_3$	0.28
$*CH_3 + H^+ + e^- \rightarrow *CH_4$	0.28

Table S17. Gibbs free energy change (Δ*G*/eV) of formationfor C–C coupling via *CO.CO, *CHO.CO, and *CH_2.CO intermediates on TM_2@BPN.

system	*CO.CO → *CO-CO	*CHO.CO → *CHO-CO	*CH_2.CO → *CH_2CO
Sc	–0.69	–1.41	—
V	0.28	0.76	—
Ni	1.65	0.81	–0.76
Cu	1.31	—	–0.34
Y	–0.69	–0.06	—
Zr	–0.30	—	—
Hf	–0.37	—	—
W	1.38	—	—
Ir	—	—	–1.33

Table S18. The values of the free energy change (ΔG/eV) at each step involved in Sc_2@BPN.

Reaction process	ΔG
$*CO + H^+ + e^- \rightarrow *CHO$	–0.03
$*CHO + CO \rightarrow *CHO.CO$	–0.45
$*CHO.CO \rightarrow *CHOCO$	–1.86
$*CHOCO + H^+ + e^- \rightarrow *CH_2OCO$	0.09
$*CHOCO + H^+ + e^- \rightarrow *CHOHCO$	0.46
$*CHOCO + H^+ + e^- \rightarrow *CHOCHO$	–0.78
$*CHOCO + H^+ + e^- \rightarrow *CHOCOH$	0.58
$*CHOCHO + H^+ + e^- \rightarrow *CH_2OCHO$	0.6
$*CHOCHO + H^+ + e^- \rightarrow *CHOHCHO$	1.06
$*CHOCHO + H^+ + e^- \rightarrow *CHOCH_2O$	0.79
$*CHOCHO + H^+ + e^- \rightarrow *CHOCHOH$	1.03
$*CH_2OCHO + H^+ + e^- \rightarrow *CH_2OHCHO$	0.48
$*CH_2OCHO + H^+ + e^- \rightarrow *CH_2OCH_2O$	–1.00
$*CH_2OCHO + H^+ + e^- \rightarrow *CH_2OCHOH$	0.51
$*CH_2OCH_2O + H^+ + e^- \rightarrow *CH_2OHCH_2O$	0.73
$*CH_2OCH_2O + H^+ + e^- \rightarrow *CH_2OCH_2OH$	1.10
$*CH_2OHCH_2O + H^+ + e^- \rightarrow *CH_3CH_2O\text{-}OH$	0.10
$*CH_2OHCH_2O + H^+ + e^- \rightarrow *CH_2OHCH_2OH$	2.11
$*CH_3CH_2O\text{-}OH + H^+ + e^- \rightarrow *OH + CH_3CH_2OH(l)$	–0.58
$*CH_3CH_2O\text{-}OH + H^+ + e^- \rightarrow *CH_3CH_2O + H_2O(l)$	–0.45
$*OH + H^+ + e^- \rightarrow *H_2O$	2.34

Table S19. The values of the free energy change (ΔG/eV) at each step involved in V_2@BPN.

Reaction process	ΔG
*CO + CO → *CO.CO	–1.01
*CO.CO → *COCO	0.28
*COCO + H^+ + e^-→ *CHOCO	0.41
*COCO + H^+ + e^- → *COHCO	1.06
*COCO + H^+ + e^- → *COCHO	–0.71
*COCO + H^++ e^- → *COCOH	1.34
*COCHO + H^+ + e^- → *CHOCHO	–0.55
*COCHO + H^+ + e^- → *COHCHO	0.89
*COCHO + H^+ + e^- → *$COCH_2O$	–0.40
*COCHO + H^+ + e^- → *COCHOH	0.85
*CHOCHO + H^+ + e^- → *CH_2OCHO	–0.44
*CHOCHO +H^+ + e^- → *CHOHCHO	0.55
*CHOCHO +H^+ + e^- → *$CHOCH_2O$	–0.05
*CHOCHO + H^+ + e^- → *CHOCHOH	0.99
*CH_2OCHO +H^+ +e^- → *CH_2OHCHO	0.75
*CH_2OCHO + H^+ + e^- → *CH_2OCH_2O	–0.42
*CH_2OCHO + H^+ + e^- → *CH_2OCHOH	1.09
*CH_2OCH_2O + H^+ + e^- → *CH_2OHCH_2O	1.37
*CH_2OCH_2O + H^+ + e^- → *CH_2OCH_2OH	1.19
*CH_2OCH_2OH + H^+ + e^- → *CH_3CH_2O-OH	–1.77
*CH_2OCH_2OH + H^+ + e^- → *CH_2OHCH_2OH	1.94
*CH_3CH_2O-OH + H^+ + e^- → *OH+CH_3CH_2OH(l)	2.08
*CH_3CH_2O-OH + H^+ + e^- → *CH_3CH_2O+H_2O(l)	1.45
*CH_3CH_2O + H^+ + e^- → *CH_3CH_2OH	2.12

Table S20. The values of the free energy change (ΔG/eV) at each step involved in Ni_2@BPN.

Reaction process	ΔG
$*CO + H^+ + e^- \rightarrow *CHO$	0.59
$*CHO + H^+ + e^- \rightarrow *CH_2O$	–0.28
$*CH_2O + H^+ + e^- \rightarrow *CH_2OH$	0.25
$*CH_2OH + H^+ + e^- \rightarrow *CH_3OH$	0.52
$*CH_2OH + H^+ + e^- \rightarrow *CH_2+H_2O(l)$	–0.20
$*CH_2 + CO \rightarrow *CH_2CO$	–0.76
$*CH_2CO + H^+ + e^- \rightarrow *CH_2CHO$	–0.61
$*CH_2CO + H^+ + e^- \rightarrow *CH_2COH$	0.05
$*CH_2CHO + H^+ + e^- \rightarrow *CH_3CHO$	0.16
$*CH_2CHO + H^+ + e^- \rightarrow *CH_2CH_2O$	0.79
$*CH_2CHO + H^+ + e^- \rightarrow *CH_2CHOH$	0.38
$*CH_3CHO + H^+ + e^- \rightarrow *CH_3CH_2O$	0.06
$*CH_3CHO + H^+ + e^- \rightarrow *CH_3CHOH$	0.30
$*CH_3CH_2O + H^+ + e^- \rightarrow *CH_3CH_2OH$	0.56

Table S21. The values of the free energy change (ΔG/eV) at each step involved in Cu_2@BPN.

Reaction process	ΔG
$*CO + H^+ + e^- \rightarrow *CHO$	0.46
$*CHO + H^+ + e^- \rightarrow *CH_2O$	–0.45
$*CHO + H^+ + e^- \rightarrow *CHOH$	0.03
$*CH_2O + H^+ + e^- \rightarrow *CH_3O$	–0.30
$*CH_2O + H^+ + e^- \rightarrow *CH_2OH$	–0.34
$*CH_2OH + H^+ + e^- \rightarrow *CH_3OH$	0.30
$*CH_2OH + H^+ + e^- \rightarrow *CH_2 + H_2O(l)$	–0.10
$*CH_2 + CO \rightarrow *CH_2CO$	–0.34
$*CH_2CO + H^+ + e^- \rightarrow *CH_3CO$	–0.30
$*CH_2CO + H^+ + e^- \rightarrow *CH_2COH$	–0.50
$*CH_2COH + H^+ + e^- \rightarrow *CH_3COH$	0.57
$*CH_2COH + H^+ + e^- \rightarrow *CH_2CHOH$	0.42
$*CH_2COH + H^+ + e^- \rightarrow *CH_2C+H_2O(l)$	0.73
$*CH_2CHOH + H^+ + e^- \rightarrow *CH_3CHOH$	–0.09
$*CH_2CHOH + H^+ + e^- \rightarrow *CH_2CH_2OH$	–0.73
$*CH_2CHOH + H^+ + e^- \rightarrow *CH_2CH+H_2O(l)$	–0.97
$*CH_2CH + H^+ + e^- \rightarrow * CH_2CH_2$	–0.12

Table S22. The values of the free energy change (ΔG/eV) at each step involved in Y_2@BPN.

Reaction process	ΔG
$*CO + H^+ + e^- \rightarrow * CHO$	–0.19
$*CHO + CO \rightarrow *CHO.CO$	–0.23
$*CHO.CO \rightarrow *CHOCO$	–0.06
$*CHOCO + H^+ + e^- \rightarrow *CHOHCO$	–0.97
$*CHOCO + H^+ + e^- \rightarrow *CHOCHO$	–2.39
$*CHOCO + H^+ + e^- \rightarrow *CHOCOH$	–0.73
$*CHOCHO + H^+ + e^- \rightarrow *CH_2OCHO$	0.59
$*CHOCHO + H^+ + e^- \rightarrow *CHOHCHO$	1.04
$*CHOCHO + H^+ + e^- \rightarrow *CHOCH_2O$	0.57
$*CHOCHO + H^+ + e^- \rightarrow *CHOCHOH$	1.09
$*CHOCH_2O + H^+ + e^- \rightarrow *CH_2OCH_2O$	–0.53
$*CHOCH_2O + H^+ + e^- \rightarrow *CHOHCH_2O$	0.53
$*CHOCH_2O + H^+ + e^- \rightarrow *CHOCH_2OH$	0.59
$*CH_2OCH_2O + H^+ + e^- \rightarrow *CH_2OHCH_2O$	0.63
$*CH_2OCH_2O + H^+ + e^- \rightarrow *CH_2OCH_2OH$	0.51
$*CH_2OCH_2OH + H^+ + e^- \rightarrow *CH_3CH_2O\text{-}OH$	–1.72
$*CH_2OCH_2OH + H^+ + e^- \rightarrow *CH_2OHCH_2OH$	2.26
$*CH_3CH_2O\text{-}OH + H^+ + e^- \rightarrow *OH + CH_3CH_2OH(l)$	1.31
$*CH_3CH_2O\text{-}OH + H^+ + e^- \rightarrow *CH_3CH_2O + H_2O(l)$	1.51
$*OH + H^+ + e^- \rightarrow *H_2O$	2.25

Table S23. The values of the free energy change (ΔG/eV) at each step involved in Zr_2@BPN.

Reaction process	ΔG
$*CO + CO \rightarrow *CO.CO$	–0.69
$*CO.CO \rightarrow *COCO$	–0.30
$*COCO + H^+ + e^- \rightarrow *CHOCO$	–1.04
$*COCO + H^+ + e^- \rightarrow *COHCO$	1.08
$*COCO + H^+ + e^- \rightarrow *COCHO$	0.50
$*COCO + H^+ + e^- \rightarrow *COCOH$	0.96
$*CHOCO + H^+ + e^- \rightarrow *CH_2OCO$	0.6
$*CHOCO + H^+ + e^- \rightarrow *CHOHCO$	0.89
$*CHOCO + H^+ + e^- \rightarrow *CHOCHO$	–0.16
$*CHOCO + H^+ + e^- \rightarrow *CHOCOH$	0.88
$*CHOCHO + H^+ + e^- \rightarrow *CH_2OCHO$	–0.13
$*CHOCHO + H^+ + e^- \rightarrow *CHOHCHO$	0.93
$*CHOCHO + H^+ + e^- \rightarrow *CHOCH_2O$	–0.12
$*CHOCHO + H^+ + e^- \rightarrow *CHOCHOH$	1.49
$*CH_2OCHO + H^+ + e^- \rightarrow *CH_2OHCHO$	0.94
$*CH_2OCHO + H^+ + e^- \rightarrow *CH_2OCH_2O$	–0.49
$*CH_2OCHO + H^+ + e^- \rightarrow *CH_2OCHOH$	1.25
$*CH_2OCH_2O + H^+ + e^- \rightarrow *CH_2OHCH_2O$	1.50
$*CH_2OCH_2O + H^+ + e^- \rightarrow *CH_2OCH_2OH$	1.37
$*CH_2OCH_2OH + H^+ + e^- \rightarrow *CH_3CH_2O.OH$	–1.96
$*CH_3CH_2O.OH + H^+ + e^- \rightarrow *OH+CH_3CH_2OH(l)$	2.01
$*CH_3CH_2O.OH + H^+ + e^- \rightarrow *CH_3CH_2O+ H_2O (l)$	2.15
$*OH + H^+ + e^- \rightarrow *H_2O$	1.37

Table S24. The values of the free energy change (ΔG/eV) at each step involved in Hf_2@BPN.

Reaction process	ΔG
CO + CO → CO.CO	–0.86
*CO.CO → *COCO	–0.37
*COCO + H^+ + e^- → *CHOCO	0.52
*COCO + H^+ + e^- → *COHCO	1.04
*COCO + H^+ + e^- → *COCHO	–1.23
*COCO + H^+ + e^- → *COCOH	1.06
*COCHO + H^+ + e^- → *CHOCHO	0.04
*COCHO + H^+ + e^- → *COHCHO	1.10
*COCHO + H^+ + e^- → *$COCH_2O$	0.63
*COCHO +H^++e^-→ *COCHOH	1.13
CHOCHO + H^+ + e^-→CH_2OCHO	–0.22
*CHOCHO + H^+ + e^-→ *CHOHCHO	1.63
*CHOCHO + H^+ + e^- → *$CHOCH_2O$	–0.21
*CHOCHO + H^+ +e^- → *CHOCHOH	1.05
*CH_2OCHO + H^+ + e^- → *CH_2OHCHO	1.07
*CH_2OCHO + H^+ + e^- → *CH_2OCH_2O	–0.65
*CH_2OCHO + H^+ + e^- → *CH_2OCHOH	1.17
*CH_2OCH_2O + H^+ + e^- → *CH_2OHCH_2O	1.81
*CH_2OCH_2O + H^+ + e^- → *CH_2OCH_2OH	1.71
*CH_2OCH_2OH + H^+ + e^- → *$CH_3CH_2O.OH$	–2.41
*CH_2OCH_2OH + H^+ + e^- → *CH_2OHCH_2OH	1.83
$CH_3CH_2O.OH$ + H^+ + e^- → OH+CH_3CH_2OH(l)	2.39
*$CH_3CH_2O.OH$ + H^+ + e^- → *CH_3CH_2O + H_2O(l)	2.50
*OH + H^+ + e^- → *H_2O	1.54

Table S25. The values of the free energy change (ΔG/eV) at each step involved in Ir_2@BPN.

Reaction process	ΔG
$*CO + H^+ + e^- \rightarrow *CHO$	0.53
$*CHO + H^+ + e^- \rightarrow *CH_2O$	0.04
$*CHO + H^+ + e^- \rightarrow *CHOH$	0.17
$*CH_2O + H^+ + e^- \rightarrow *CH_2OH$	0.26
$*CH_2OH + H^+ + e^- \rightarrow *CH_2+H_2O(l)$	–0.12
$*CH_2 + CO \rightarrow *CH_2CO$	–1.33
$*CH_2CO + H^+ + e^- \rightarrow * CH_2CHO$	–0.05
$*CH_2CO + H^+ + e^- \rightarrow *CH_2COH$	0.09
$*CH_2CHO + H^+ + e^- \rightarrow *CH_3CHO$	0.25
$*CH_2CHO + H^+ + e^- \rightarrow *CH_2CH_2O$	–0.03
$*CH_2CHO + H^+ + e^- \rightarrow *CH_2CHOH$	0.41
$*CH_2CH_2O + H^+ + e^- \rightarrow *CH_3CH_2O$	–0.09
$*CH_2CH_2O + H^+ + e^- \rightarrow *CH_2CH_2OH$	0.20
$*CH_3CH_2O + H^+ + e^- \rightarrow *CH_3CH_2OH$	0.59

Table S26. The PDS and ΔGmax (eV) for products of CH_4, CH_3OH, CH_2CH_2, and CH_3CH_2OH on TM_2@BPN.

Systems	PDS	ΔG_{max}	Products
Sc_2@BPN	$*CH_3O \rightarrow *CH_3OH$	2.34	CH_3OH
	$*OH \rightarrow *H_2O$	2.39	CH_4
	$*OH \rightarrow *H_2O$	2.34	CH_3CH_2OH
Ti_2@BPN	$*CH_3O \rightarrow *CH_3OH$	2.17	CH_3OH
	$*OH \rightarrow *H_2O$	2.17	CH_4
V_2@BPN	$*CH_3O \rightarrow *CH_3OH$	2.47	CH_3OH
	$*OH \rightarrow *H_2O$	2.27	CH_4
	$*CH_3CH_2O \rightarrow *CH_3CH_2OH$	2.12	CH_3CH_2OH
Mn_2@BPN	$*CH_3O \rightarrow *CH_3OH$	1.52	CH_3OH
	$*OH \rightarrow *H_2O$	2.13	CH_4
Fe_2@BPN	$*CH_2OH \rightarrow *CH_3OH$	1.03	CH_3OH
	$*CH_3 \rightarrow *CH_4$	0.62	CH_4
Ni_2@BPN	$*CO \rightarrow *CHO$	0.59	CH_3OH
	$*CH_3 \rightarrow *CH_4$	0.67	CH_4
	$*CO \rightarrow *CHO$	0.59	CH_3CH_2OH
Cu_2@BPN	$*CO \rightarrow *CHO$	0.46	CH_3OH
	$*CH_3 \rightarrow *CH_4$	0.61	CH_4
	$*CO \rightarrow *CHO$	0.46	CH_2CH_2
Y_2@BPN	$*CH_3O \rightarrow *CH_3OH$	1.90	CH_3OH
	$*OH \rightarrow *H_2O$	2.25	CH_3CH_2OH
Zr_2@BPN	$*CH_3CH_2.OH \rightarrow *OH$	2.01	CH_3CH_2OH

Nb_2@BPN	$*CH_3O \rightarrow *CH_3OH$	1.37	CH_3OH
Hf_2@BPN	$*CH_3CH_2.OH \rightarrow *OH$	2.39	CH_3CH_2OH
Ta_2@BPN	$*OH \rightarrow *H_2O$	1.35	CH_4
W_2@BPN	$*CH_3O \rightarrow *CH_3OH$	0.89	CH_3OH
	$*CH_2\text{-}OH \rightarrow *CH_2$	1.65	CH_4
Ir_2@BPN	$*CO \rightarrow *CHO$	0.53	CH_3OH
	$*CO \rightarrow *CHO$	0.53	CH_4
	$*CH_3CH_2O \rightarrow *CH_3CH_2OH$	0.59	CH_3CH_2OH

Table S27. The products and U_L for CORR on the selected Fe_2@BPN, Ni_2@BPN, Cu_2@BPN, and Ir_2@BPN in this work and the other systems in previous reports for comparison.

Systems	Products	U_L
Fe_2@BPN	CH_4	–0.62
Ir_2@BPN	CH_4	–0.53
Ni_2@BPN	CH_3CH_2OH	–0.59
Cu_2@BPN	CH_2CH_2	–0.46
B_2@Bi[1]	CH_4	–0.57
$Ru_2@C_2N$[2]	CH_4	–0.58
Mn_2@Pc[3]	CH_4	–0.84
Cu (100)[4]	CH_2CH_2	–0.72
$Cu_4@C_5N_2H_2$[5]	CH_2CH_2	–0.50
$Fe_2@C_2N$[6]	CH_2CH_2	–0.76
B@GRY[7]	CH_3CH_2OH	–0.53
Cu_2B_2[8]	CH_3CH_2OH	–0.59
$Cu_4@C_2N$[9]	CH_3CH_2OH	–0.81

1. Y. Meng, Z. Xu, Z. Shen, Q. Xia, Y. Cao, Y. Wang and X. Li, *Journal of Materials Chemistry A*, 2022, **10**, 6508-6522.
2. X. Cui, W. An, X. Liu, H. Wang, Y. Men and J. Wang, *Nanoscale*, 2018, **10**, 15262-15272.
3. H. Shen, Y. Li and Q. Sun, *The Journal of Physical Chemistry C*, 2017, **121**, 3963-3969.
4. S. Hanselman, M. T. M. Koper and F. Calle-Vallejo, *ACS Energy Letters*, 2018, **3**, 1062-1067.
5. D. Zhang, O. V. Prezhdo and L. Xu, *Journal of the American Chemical Society*, 2023, **145**, 7030-7039.
6. H. Liu, Q. Huang, W. An, Y. Wang, Y. Men and S. Liu, *Journal of Energy Chemistry*, 2021, **61**, 507-516.
7. P. Mano, S. Namuangruk and K. Takahashi, *The Journal of Physical Chemistry C*, 2023, **127**, 7683-7694.
8. J. Jia, H. Zhang, Z. Wang, J. Zhao and Z. Zhou, *Journal of Materials Chemistry A*, 2020, **8**, 9607-9615.
9. Y. Wang, N. Ma, Y. Zhang, B. Liang and J. Fan, *Applied Surface Science*, 2023, **626**.